MSc thesis in Civil Engineering

The optimization design reinforcement for Diaphragm Wall

Wei Xiaoyan

2024

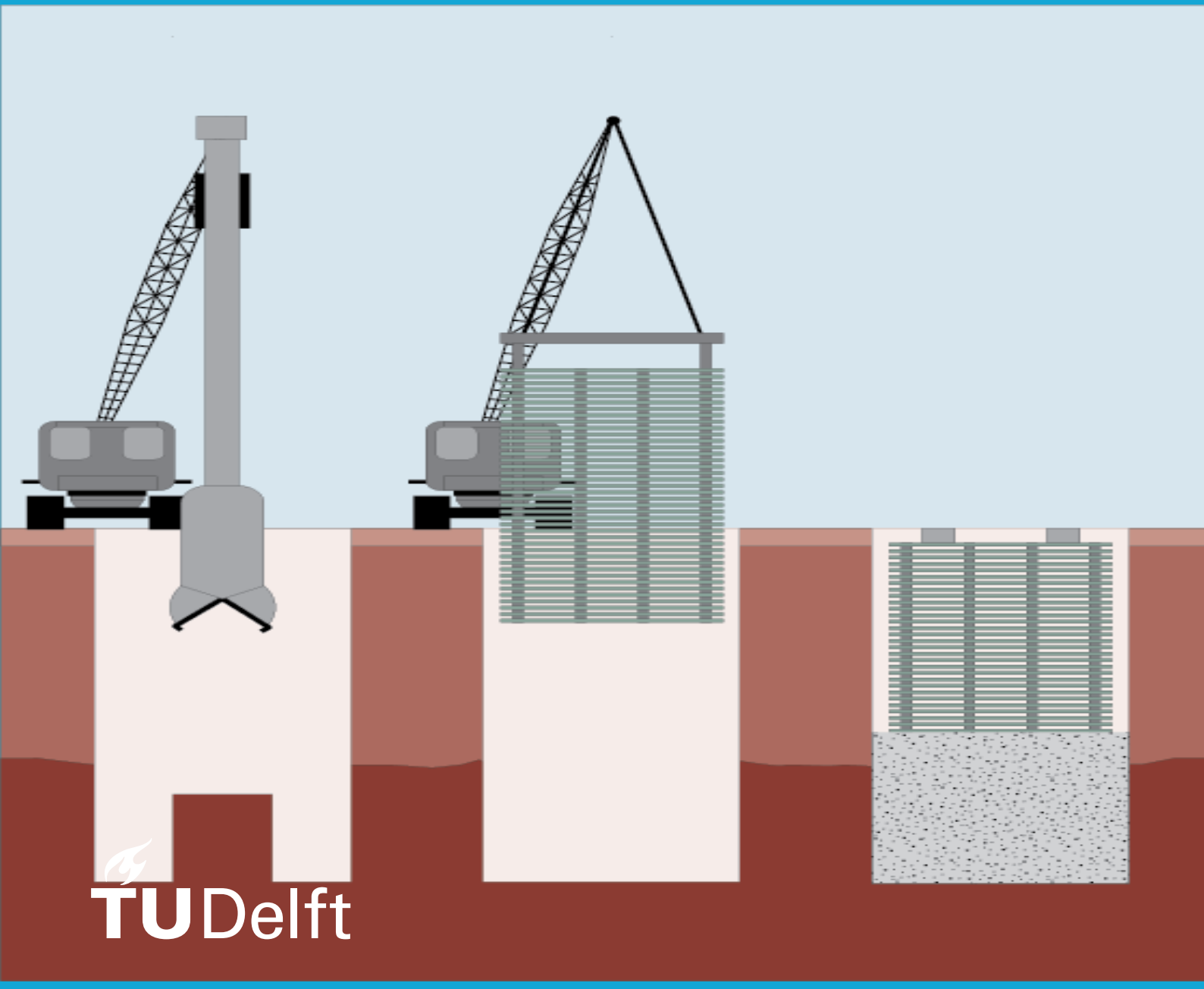

TU Delft

MSc thesis in Civil Engineering

Optimization of reinforcement design for Diaphragm wall

Wei Xiaoyan

November 2024

A thesis submitted to the Delft University of Technology in partial fulfillment of the requirements for the degree of Master of Science in Civil Engineering

Wei Xiaoyan: *Optimization of reinforcement design for Diaphragm wall* (2024)

The work in this thesis was carried out in the:

Abstract

Diaphragm walls are commonly used in civil engineering for their versatility, serving as structural support, reducing ground movement, and providing waterproofing. This research explores how soil and concrete interact at the interface of diaphragm walls, emphasizing both structural and geotechnical aspects. A non-linear analysis approach is proposed to assess the Ultimate Limit State (ULS) and Serviceability Limit State (SLS) of diaphragm walls, aiming to optimize their reinforced concrete design. By utilizing Diana software, various scenarios are modeled to improve the efficiency and reliability of diaphragm wall construction while ensuring safety.

Despite the growing popularity of diaphragm walls, there is still a lack of understanding regarding soil-concrete interaction and nonlinear behavior analysis for combining the soil and concrete part, which hinders the optimization of reinforced concrete design. This study aims to fill that gap by refining reinforced concrete design and ensuring structural integrity during construction without compromise the safety philosophy. The primary objectives are to enhance the efficiency, reliability, and sustainability of diaphragm walls through a thorough analysis of soil-concrete interactions and nonlinear behaviors.

Key research questions focus on how non-linear analysis influences structural design, the differences in bending moment distribution between linear and non-linear analyses, and the benefits of incorporating soil-concrete interaction into reinforcement design. By shedding light on diaphragm wall construction, this research seeks to create a balanced design that emphasizes safety, cost-effectiveness, and efficiency, ultimately leading to more sustainable construction practices.

Acknowledgements

Thank you to everyone, especially my supervisors, family, and friends.

I am deeply grateful to my family for their unwavering support, which allowed me to complete my thesis and studies with joy. I appreciate my advisor for not only providing significant academic guidance but also offering invaluable life advice. A heartfelt thank you goes to my friends for their companionship, joy, and encouragement throughout this journey. I also want to acknowledge my own perseverance.

I extend my gratitude to my colleagues who check in on me during times of confusion, as well as to everyone who has brightened my days with a simple "How are you?" I feel fortunate for all these connections. This brief conclusion marks a new beginning, and I am thankful for the profound experiences that have given me fresh insights into life

...

Contents

List of Figures

List of Tables

1. Introduction

1.1. Research Context

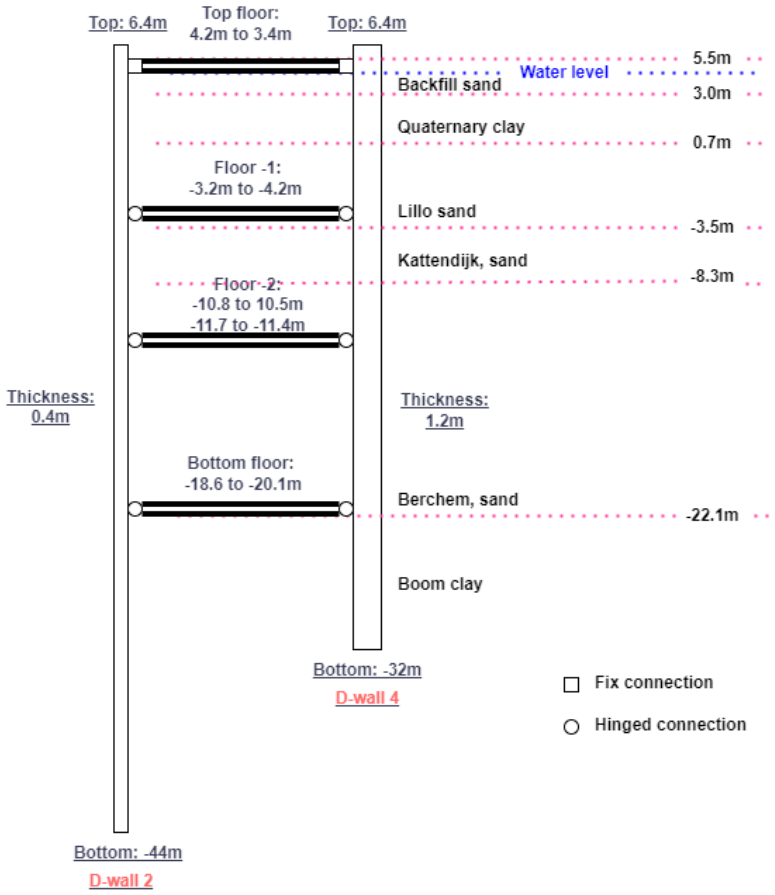

Figure 1.1.: Simplified geometry for D-wall

Diaphragm walls are widely used in the civil engineering industry to address various construction challenges, such as providing structural support as retaining or foundation walls, minimizing ground movement, and ensuring waterproofing. Currently, the practical case design relies solely on linear analysis, considering only the reduction of concrete stiffness (20GPa) for reinforced concrete design. In principle, this approach may be over conservative, leading to designs that are neither sustainable nor cost-effective. There is a significant gap remains in incorporating nonlinear concrete and soil analyses to achieve a more refined and accurate design. This research explores the combined effects of nonlinear soil and concrete analyses on the design process while also considering the fully nonlinear effects of soil-structure interaction.

This research focuses on an example of practical case as Figure 1.1 shows the involving a diaphragm wall (D-wall 4) involving a heavily reinforced diaphragm wall (D-wall 4) within a tunnel section. Table 1.1 indicates the reinforcement is very heavy in D-wall 4, aiming to enhance the reinforced concrete design for D-wall 4.

Table 1.1.: D-wall final reinforcement design

D-wall Design	
Thickness	**1.2m**
Concrete type	**C35/45**
Concrete stiffness	**34077 MPa**
C_{app}	**100mm**
Longitudinal reinforcement	
Tunnel side	**283mm@50+283mm@40**
Ground side	**283mm@40+283mm@50**
Shear reinforcement	
Depth(m)	Reinforcement
3-0	275mm-@20
0- (-10)	150mm-@20
-10 - (-15)	100mm-@20
-15 - (-20)	250mm-@20
-20 - (-25)	150mm-@20

The study begins with a simplified case analysis to understand the mechanical processes, which is then applied to improve the reinforced concrete design of the practical case.

Utilizing DIANA software, the research models various scenarios with the ultimate goal of optimizing the design of diaphragm wall reinforcement. The findings aim to result in more economical and sustainable construction plans by enhancing the reinforced concrete design of diaphragm walls.

1.2. Research questions

Main question:

- How does the combination of nonlinear analysis for both concrete and soil affect the structural design of reinforced concrete Diaphragm walls?

Sub question:

- What are the key differences in bending moment distribution between linear and nonlinear concrete analysis?
- What are the key differences in soil concrete interaction between linear and nonlinear concrete analysis?
- How does nonlinear analysis and soil-concrete interaction enhance reinforcement design, and what key advantages does it offer?

2. Literature review

2.1. Diaphragm wall background information

- Function of D-wall

A concrete diaphragm wall, or slurry wall, is an underground structure made of panels, used as a foundation or retaining wall. It prevents water from entering excavation sites and can reduce noise and vibrations, benefiting nearby buildings and residents.The Constructor, 2021.

- Construction of D-wall

The construction stage of diaphragm wall:
1. Guide wall construction
2. Excavation
3. Installation of reinforcement cage and concreting the trench
4. Joints installation
D-wall construction is done panel-by-panel, starting with a guide wall for alignment and soil support.

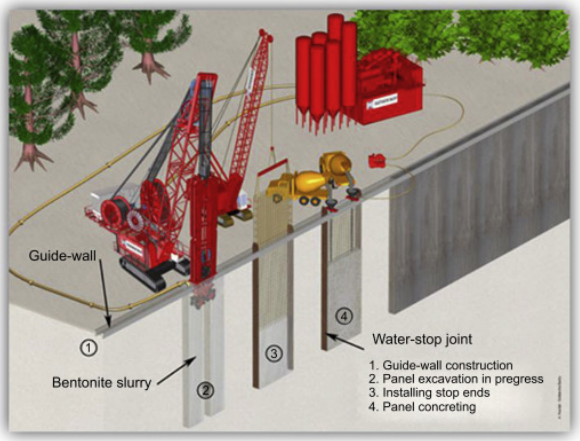

Figure 2.1.: D-wall construction procedure Singh, 2023

Primary panels are excavated first, followed by secondary ones. Reinforcement is added, then concrete is poured via tremie pipes. Panels are connected with joints to ensure structural integrity.

2.2. Soil-structure interaction

This section focuses on the soil structure interaction (SSI) of diaphragm wall, highlighting the interaction between the wall and soil. The key element are show in Figure 2.2.

2.2.1. Interaction elements

The discussion about soil structure interaction refers to the soil, wall and mainly the movement between the soil and wall as Figure 2.2.

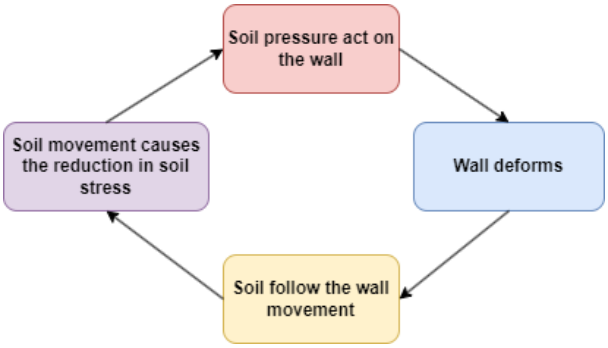

Figure 2.2.: Soil structure interaction element

- Soil pressure

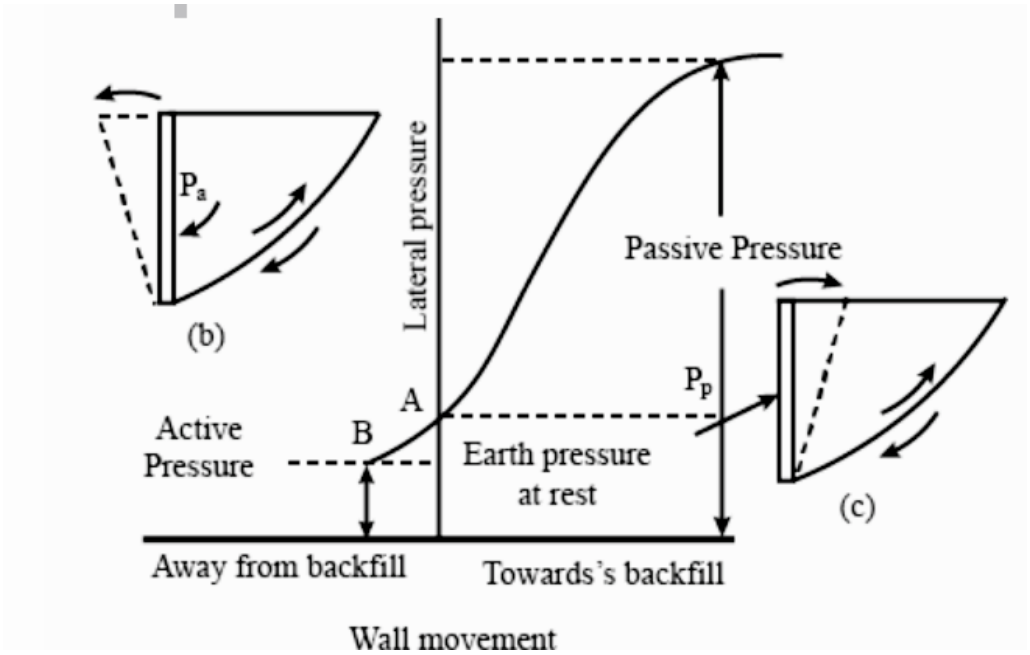

Figure 2.3.: Wall displacement vs Lateral soil pressure

The at-rest earth pressure is an assumed state where the soil and the structure are assumed to **never** move Frame, 2024. This concept is typically applied under static conditions, especially when dealing with very large or extensive D-walls. At-rest pressure is relevant when the wall does not undergo any lateral movement. It is assumed that extremely large and heavy structures reaching down to bedrock are static; therefore, at-rest pressure can be used to calculate the force exerted by the soil on such structures.
Active Pressure: Minimum lateral stress as the wall moves away, causing soil shear failure.
Passive Pressure: Maximum lateral stress as the wall pushes into the soil, also leading to shear failure.

As the discussed above and shown in 2.3, three lateral soil pressures are considered: active, passive, and at-rest. During soil-structure interaction, if the soil fails, it moves with the diaphragm wall, maintaining the same lateral pressure (active/passive pressure). However, if the soil does not fail, the movement occurs between the active and passive pressures, and the lateral soil pressure is influenced by the movement of the diaphragm wall. Because the X-axis is the wall movement shows in the Figure

2.3, In this scenario, the soil movement closely follows the diaphragm wall movement, despite the friction between the wall and the soil. This relationship means that the wall movement significantly influences the lateral soil pressure, as indicated on the Y-axis.

- Wall movement

As discussed above, soil pressure is influenced by the displacement of the diaphragm wall (D-wall), with concrete stiffness playing a crucial role in determining wall movement. A softer wall permits greater movement, while a stiffer wall restricts it. Figure 2.3 illustrates these two scenarios:

The wall moves away from backfill, and wall moves towards the backfill, which determined the soil is unloaded or loaded.

Unloaded Soil: A stiffer wall leads to less deformation, resulting in increased lateral pressure. Conversely, a softer wall allows more deformation, which reduces lateral pressure.
Loaded Soil: A stiffer wall minimizes movement and lateral pressure, while a softer wall results in greater displacement and higher lateral pressure.

- Concrete stiffness

After establishing that wall displacement is directly influenced by concrete stiffness, nonlinear concrete analysis models cracks with reduced stiffness in cracked areas compared to uncracked regions. In practice, reinforcement design uses a reduced concrete stiffness in linear analysis, typically set at 60 percent of the original stiffness. For C35/45 concrete, this reduction brings stiffness down to 20 GPa, accounting for the overall reduced stiffness of the D-wall concrete.

While linear analysis provides an average reduced stiffness, nonlinear analysis targets specific crack locations, offering a more accurate depiction of crack stiffness, which is typically lower stiffness in those crack zones.

Consequently, greater displacement may occur in cracked areas because of lower stiffness, leading to changes in the lateral soil pressure acting on the diaphragm wall (D-wall).

To validate this, three analyses will be conducted: a linear analysis with reduced concrete stiffness, a linear analysis with original concrete stiffness, and a nonlinear analysis. These analyses will enable a comparison of soil-structure interaction and the impact of nonlinear analysis on design.

2.3. Design of Diaphragm wall

This section reviews diaphragm wall design methods, comparing each to identify the best fit for this research. The three main methods are:
Analytical model (Blum, 1931)
Spring model (1975)
Finite Element model (1985)

- Analytical model

The analytical model (BLUM method) is the oldest design method for retaining walls, using the limit equilibrium method (LEM) developed by Blum in 1931. LEM assumes maximum active and passive soil pressures at failure but doesn't account for wall displacement, making it not suitable for analyzing the soil structure interaction. Ilieş et al., 2015. Figure 2.4 shows a self-supporting wall below excavation level, resisting soil pressure through stiffness. The Limit Equilibrium Method estimates maximum wall height, assuming linear soil pressure and rotation at a fixed point, but BLUM's uniform pressure assumption may not match real-world conditions.

- Spring model

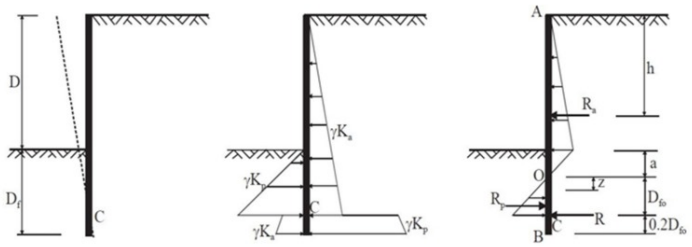

Figure 2.4.: Limit Equilibrium Method for D-wall

The spring model, or subgrade reaction modulus method (SRM), uses a "subgrade reaction modulus" to represent soil-structure interaction with elastic supports, typically elastic-plastic springs. The wall is modeled as a one-dimensional elastic beam. Popular software for simulating D-wall behavior includes D-sheet piling and Diana, both of which use the spring model Ilieş et al., 2015.

A comparison Zhou, 2015 between D-Sheet piling and Plaxis 2D shows that D-Sheet piling only analyzes D-wall behavior, while Plaxis models both soil and structure reactions. This highlights a major disadvantage of the spring model: it can simulate soil-structure interaction but cannot analyze soil deformation, such as the surface soil settlements.

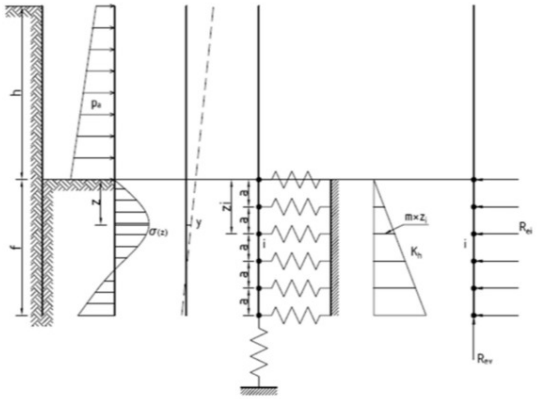

Figure 2.5.: The spring model

- Finite Element model

The Finite Element Model (FEM) is the third design option, predicting initial and changing stresses and strains during construction. It enhances design accuracy by considering soil-structure interaction and is useful for risk control. Comparisons Zhou, 2015 show that PLAXIS offers more comprehensive results than D-sheet piling, including soil and structure deformation. However, FEM requires fast computers and can be more costly than the spring model.

To conduct a more detailed analysis of soil and structural behavior in this research, including nonlinear concrete behavior and soil-structure interaction with soil and wall displacement, a Finite Element Model be employed.

2.4. Non-linear behavior for structural and geotechnical analysis

This section in order to introduce the soil and concrete non-linear model for analysing D-wall behavior. Additionally, many different parameters for soil and concrete are present which are related to the models.

1. Soil non-linear analysis:

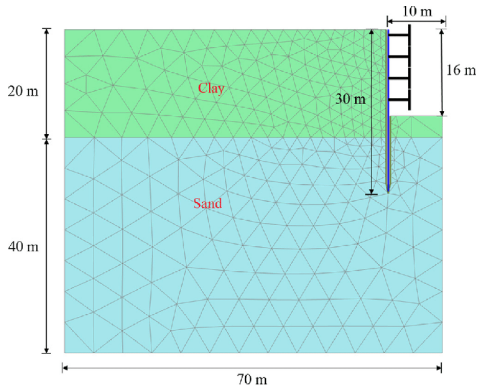

Figure 2.6.: Finite element method model Wu et al., 2022

Hardening Soil Model with Small-Strain Stiffness (HSsmall): An advanced elastoplastic model that accounts for stress-dependent stiffness and shear hardening is widely used for numerical excavation analysis. This model explains how soil stiffness increases with load and can accumulate plastic strain prior to soil failure. It also differentiates between loading and unloading stiffness, accurately reflecting soil behavior during excavation. Additionally, strain-dependent stiffness is incorporated to capture soil behavior under small strain conditions.

2. Structural Non-Linear Analysis

Linear elastic Model: The Linear Elastic Model in DIANA is chosen based on the project type. It's often used for tunnel linings and simulates concrete behavior when it is mostly elastic. A
Multi-directional Fixed Crack Model: The Multi-Directional Fixed Crack Model simulates cracking in structures using smeared cracking. It includes tension softening and shear retention. This model works well for tensile cracking but does not account for compressive behavior Chai, 2020. **Total Strain-Based Crack Models**: The Total Strain-Based Crack Model is commonly used for modeling non-linear concrete behavior. It looks at cracking direction and includes tensile, shear, and compressive behavior Chai, 2020.
Rankine principal stress model: The Rankine Principal Stress Model simulates smeared cracking, focusing on biaxial compression in 2D. It shows how pressure in one direction affects stress in another direction.

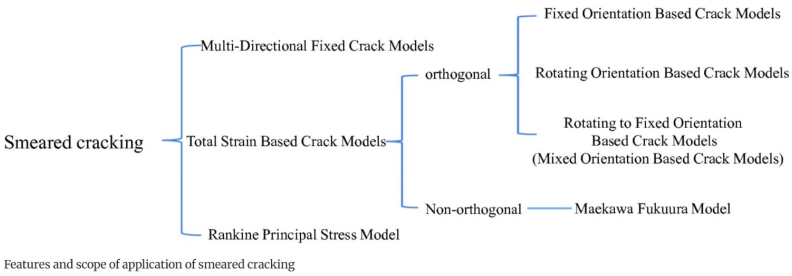

Figure 2.7.: The different types of model used for smeared cracking simulation Chai, 2020

This research utilizes the total strain-based rotating crack model to analyze nonlinear concrete behavior, as suggested in Research and Technical Development, 2022. For linear analysis, a linear elastic model is applied to represent the concrete's linear behavior.

- Reinforcement model:

Embedded reinforcement modelling: The Embedded Reinforcement Model simulates a lot of reinforcement and uses bond-slip properties specific to the embedded reinforcement. It doesn't move freely; its stiffness depends on the positions of the reinforcement and concrete elements. This model

also needs details like diameter and spacing. Using this model simplifies the process because it doesn't require changing how the concrete elements connect. Hendriks and Roosen, 2022.

Bond-Slip Models: Bond-Slip Models are used for detailed analysis of how concrete interacts with reinforcement. They help predict crack widths in reinforced concrete, which is essential for applying the bond-slip model. However, these models only work with regular plane stress, curved shell, or solid elements that use linear or quadratic interpolation.

In this research, due to the high density and high diameter of reinforcement in the practical example, the embedded reinforcement model is used, without accounting for bond-slip between the concrete and reinforcement.

2.5. Safety philosophy for D-wall

- Ultimate Limit state:

Ultimate limit state (ULS): The Ultimate Limit State (ULS) is important for designing structures. It refers to the point where a structure can no longer support the loads it was designed for, leading to failure. This can happen due to issues like buckling, plastic deformation, or fractures, which cause the structure to lose its strength and stiffness.

The Ultimate Limit State (ULS) design in Eurocode 2 is crucial for making sure structures can handle maximum bending, shear, torsion, and punching forces without collapsing. It includes designing for strut and tie models, anchorage, lap joints, partially loaded areas, and fatigue. This approach considers potential problems and offers solutions to ensure the structure's safety and stability.

In *Eurocode 7: Geotechnical Design - Part 2: Ground Investigation and Testing*, 1997-2:2007, there are several specific limits state to check the ULS is achieved for geotechnical aspect: **1. EQU:** Loss of balance in the structure or ground, treating them as rigid bodies without considering material strength.
2.STR: Internal failure or too much deformation in the structure or its parts.
3.GEO : Failure or excessive deformation of the ground, affecting the sizing of foundations or retaining structures.
4.UPL: Loss of balance due to uplift from buoyancy or other vertical forces.
5.HYD: Issues like hydraulic heave, internal erosion, and piping caused by water movement in the ground.

For the STR and GEO limit states in both normal and temporary situations, there are three design approaches to determine the partial factors for:
Actions (A): The effects of loads.
Material properties (M): The characteristics of materials.
Resistance (R): The ability to withstand loads.
The differences between these approaches highlight uncertainties in how we model the effects of actions and resistance.
Design approach 1: Except for design of axially loaded pile and anchors:
Combination 1: A1 ″+″ M1 ″+″ R1
Combination 2: A1 ″+″ M2 ″+″ R1 (where ″+″ implies to be combine with)
For Combination 1 and 2, the partial factor are applied to action or effect of action, and to the ground strength.
For designing of axially loaded piles and anchors:
Combination 1: A1 ″+″ M1 ″+″ R1
Combination 2: A1″+″ (M1 or M2) ″+″ R1
M1: is used for calculating of piles or anchors. M2: for calculating the unfavourable action.
For Combination 1, the partial factor applied to actions and ground strength parameters. For Combination 2, the partial factor applied to actions, ground strength resistance and sometimes to ground strength parameter.
Design approach 2: A1 ″+″ M1 ″+″ R2

The partial factors are applied to actions and to ground resistance.
Design approach 3: ($A1^*$ or $A2^+$) "+" M2 "+" R3
$A1^*$: on structural actions. $A2^+$: on geotechnical action.
The partial factors are applied to action / effects of actions from the structure and to ground strength parameters.

In the Netherlands, the commonly used design approach is DA3.

- Serviceability Limit state:

Serviceability limit state (SLS): To satisfy an actual engineering design, Serviceability limit state (SLS) is an essential computation check. This state requires a structure must maintain functionality for its intended purpose under regular (daily) loads, and therefore should not cause discomfort to occupants during normal conditions.

In Eurocode 2 for Standardization, 2004, the serviceability limit state mainly focus on three aspect: **stress limitation**, **crack control**, and **deflection control**. For verifications of stress state and deflection the value can be directly read from the non-linear finite element analysis and compared with the limit values imposed by the current codes Allaix, 2020. And for the for the cracks opening should be calculates as:
$w = S_{r,max} * \varepsilon_s$
Where ε_s is the average strain value of the longitudinal reinforcement in the cracked zone from the analysis. And $S_{r,max}$ is the maximum cracking spacing.

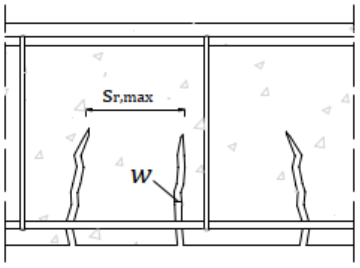

Figure 2.8.: Longitudinal crack Hendriks and Roosen, 2022

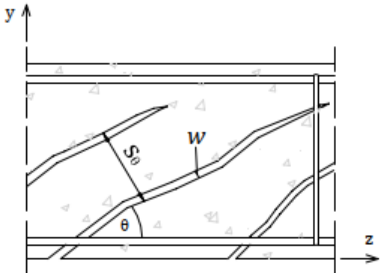

Figure 2.9.: Shear crack Hendriks and Roosen, 2022

In this three main stages, Eurocode 2 proposes a method to calculate criteria to limit and control, aiming to ensure that the structure does not compromise the usability and appearance of the structure. In addition, Eurocode 2 for SLS design incorporates second-order effects and classifies composite cross-sections Yorsa et al., 2012. The SLS ensures that a structure not only remains standing but also remains fit for use and endurable throughout its intended lifespan.

An analysis that accounts for the nonlinear behavior of concrete and soil reveals that cracking in the foundation alters the soil's failure mechanism Gajo, 2023. From that, it could be said the crack happen for D-wall could also influence the nearby soil failure mechanism.

3. Case study

In order to have better understanding of the influence of nonlinear concrete and soil-structure interaction between the soil and D-wall, the simple case first discussed. The geometry of the case study is shown in Figure 3.1.

3.1. Geometry

The cross-section for modeling the diaphragm wall is shown in Figure 3.1. The first three sand layers represent the corresponding layers from the practical case first three sand layer, ensuring comparability. Notably, there is no water present in the model. The wall thickness in the case study is 0.5 m to allow for adequate reinforcement placement within the concrete, and the length of the diaphragm wall is 16.5 m. Additionally, only one strut is included in the case study.

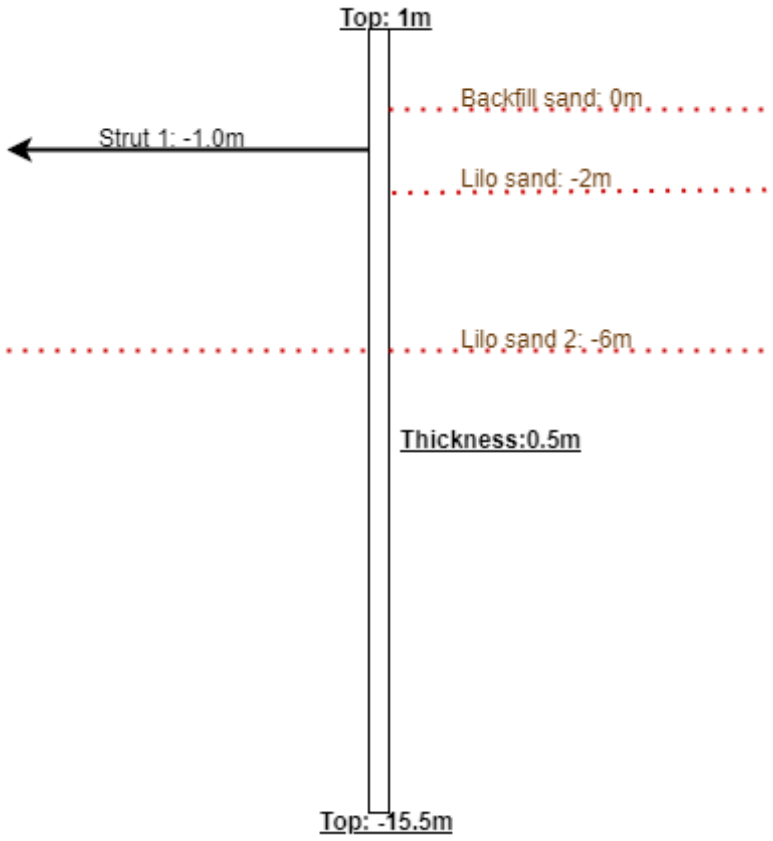

Figure 3.1.: Case study cross section for D-wall

In addition to the description above, the adaptation of the **material and the element**, concrete, the strut, and the information of specific details for the soil are totally the same as in the Appendix A demonstration, to make the case study comparable for practical case. And for the case study, there is no floor. The soil index shows in Table 3.1, the interface index shows in Table 3.2.

For this case study, there is no load for each construction stage.

Table 3.1.: Soil Layers and Properties for case study

No.	Soil Type	Top of the layer (mNAP)	γ (kN/m^3)	ϕ^* (°)	ψ^* (°)
1	Backfill sand	1.0	18.0	32.5	0
2	Lillo 1, sand	-2.0	16.5	30	2
3	Lillo 2, sand	-6.0	16.5	35	5

Table 3.2.: Properties of interface parameters

Type of Soil	Normal Stiffness (KPa/m)	Shear Stiffness (KPa/m)	Cohesion (KPa)	Friction Angle (°)
Backfill sand	1.00×10^9	2000	0	15
Lillo 1, sand	1.00×10^9	2000	0	15
Lillo 2, sand	1.00×10^9	2000	0	15

Table 3.3.: Construction Stages for case study

No.	Construction Phase
1	Geostatic (before D-wall apply)
2	Install D-wall
3	Excavate to -2m
4	Installation strut 1
5	Excavation to -8.5m

After done the sensitivity analysis shows in Appendix B for the case study FEM , before starting the analysis, the following setting is determined:

Table 3.4.: The analysis setting

Mesh size for D-wall	0.1m
Load step for analysis	Load type 4 (see Appendix B)
Iteration times	50

After the sensitivity analysis for the mesh size, the mesh size is determined to be as Figure 3.2.

And the determined reinforcement design is shown Table 3.5, the reinforcement design check is shown in Appendix B.

Table 3.5.: D-wall Final Design for Case Study

D-wall Design	
Thickness	**0.5m**
Concrete type	**C35/45**
Reinforcement Design	
Minimum required coverage C_{min}	**45mm**
Applied coverage C_{nom}	**50mm**
Excavation side reinforcement	**@20(150mm)**
Ground side reinforcement	**@20(315mm)**

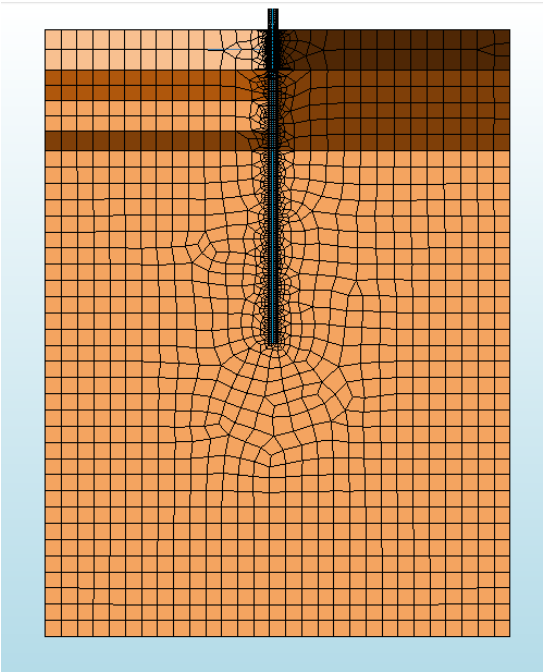

Figure 3.2.: Final mesh for case study

3.2. Bending moment distribution result

After deciding all information for case study, three analyses are conduct:
1.**L34:** Soil nonlinear analysis and concrete linear analysis with original concrete stiffness (green line)
2. **L20:** Soil nonlinear analysis and concrete linear analysis with reduced concrete stiffness (Grey line)
3. **NL:**Soil nonlinear analysis and concrete nonlinear analysis with original concrete stiffness (Red line)
First, the results of three analysis bending moment distribution is shows as follows:

From the Figure 3.3, the -8.5m is the excavation depth. Above the excavation depth, the peak bending moment value occurs on the negative side:

Linear analysis with original concrete stiffness (L34) $>$ Linear analysis with reduced concrete stiffness (L20) $>$ Nonlinear analysis with original concrete stiffness (NL)

Shows the minimum peak value for bending moment distribution is the fully nonlinear analysis. However, below the excavation depth, the bending moment peak value (positive bending moment peak value):

Linear analysis with original concrete stiffness (L34) $<$ Linear analysis with reduced concrete stiffness (L20) $<$ Nonlinear analysis with original concrete stiffness (NL)

For below the excavation depth, the bending moment peak value shows completely opposite result.

In Figure 3.3, the yellow line denotes the concrete's cracking moment threshold. Above the excavation depth, the positive side bending moment peak is below this threshold, indicating no cracking in that region. Below the excavation depth, the red line (NL) bending moment values also stay within cracking limits, confirming no cracking there either. Conversely, on the negative side above the excavation, the bending moment exceeds the cracking moment, indicating cracking. Thus, cracking occurs primarily above the excavation depth, while below it, no cracking is observed.

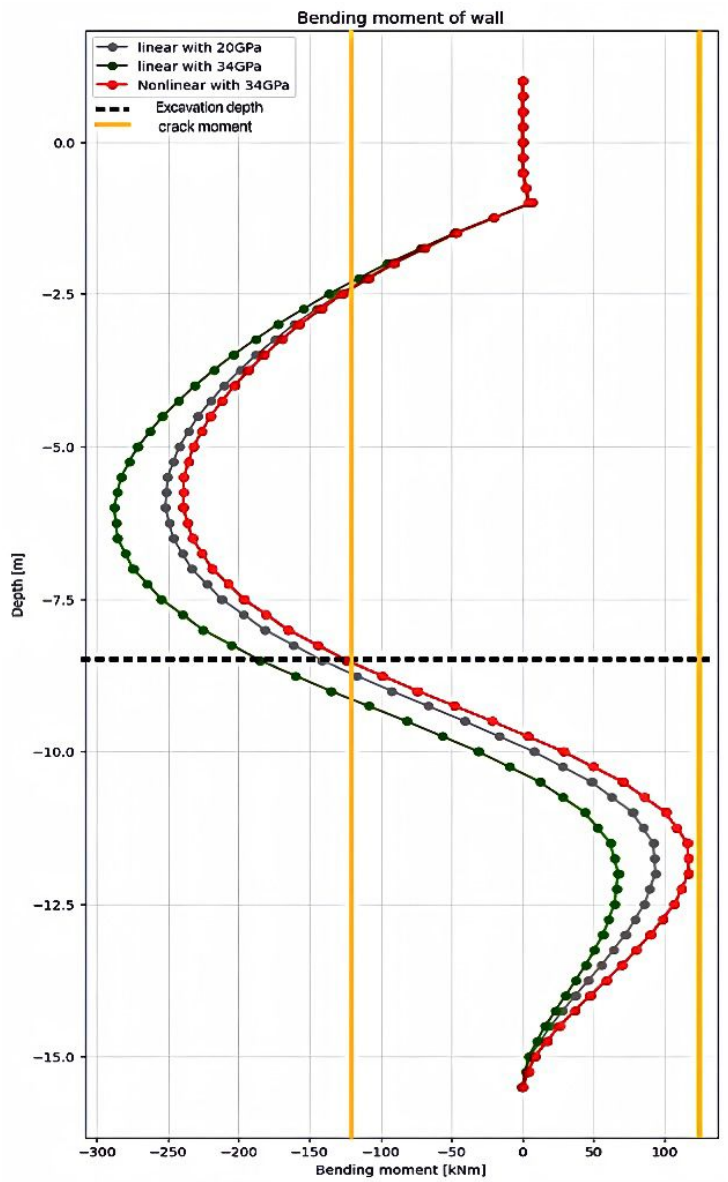

Figure 3.3.: Bending moment distribution for three analysis

3.3. Wall displacement result

Figure 3.4 shows the three analysis wall displacement, still the -8.5m is the excavation depth. Above the excavation depth, the wall displacement shows:

Linear analysis with original concrete stiffness (L34) $<$ Linear analysis with reduced concrete stiffness (L20) $<$ Nonlinear analysis with original concrete stiffness (NLA)

Above the -8.5m, it shows the nonlinear concrete analysis has the largest result for wall horizontal displacement compared to other two concrete linear analysis.

Below the excavation depth (-8.5m):

Linear analysis with original concrete stiffness (L34) $>$ Linear analysis with reduced concrete stiffness (L20) $\approx$ Nonlinear analysis with original concrete stiffness (NLA)

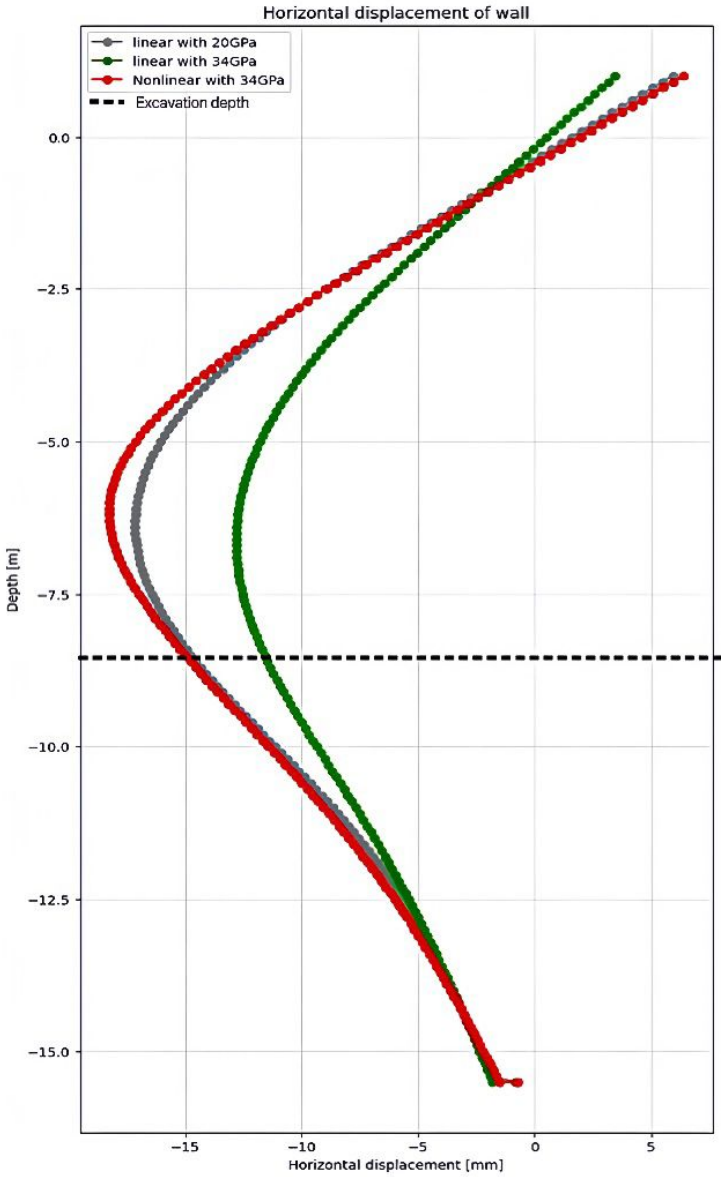

Figure 3.4.: Wall displacements for different three analysis

Below the -8.5m, it shows the nonlinear concrete analysis result for wall horizontal displacement is very close to the linear concrete reduced stiffness analysis result.

Additionally, the displacement results from the three analyses indicate that the wall still shows a slight inclination near the bottom, below the excavation depth. This suggests that the wall may not be embedded deeply enough to provide full stability.

3.4. Soil pressure result

3.4.1. Total soil pressure

Figure 3.5 presents the soil pressure results from three analyses acting on the diaphragm wall (D-wall). Some areas exhibit significant differences among the three analyses, while other regions show overlapping results across all analyses.

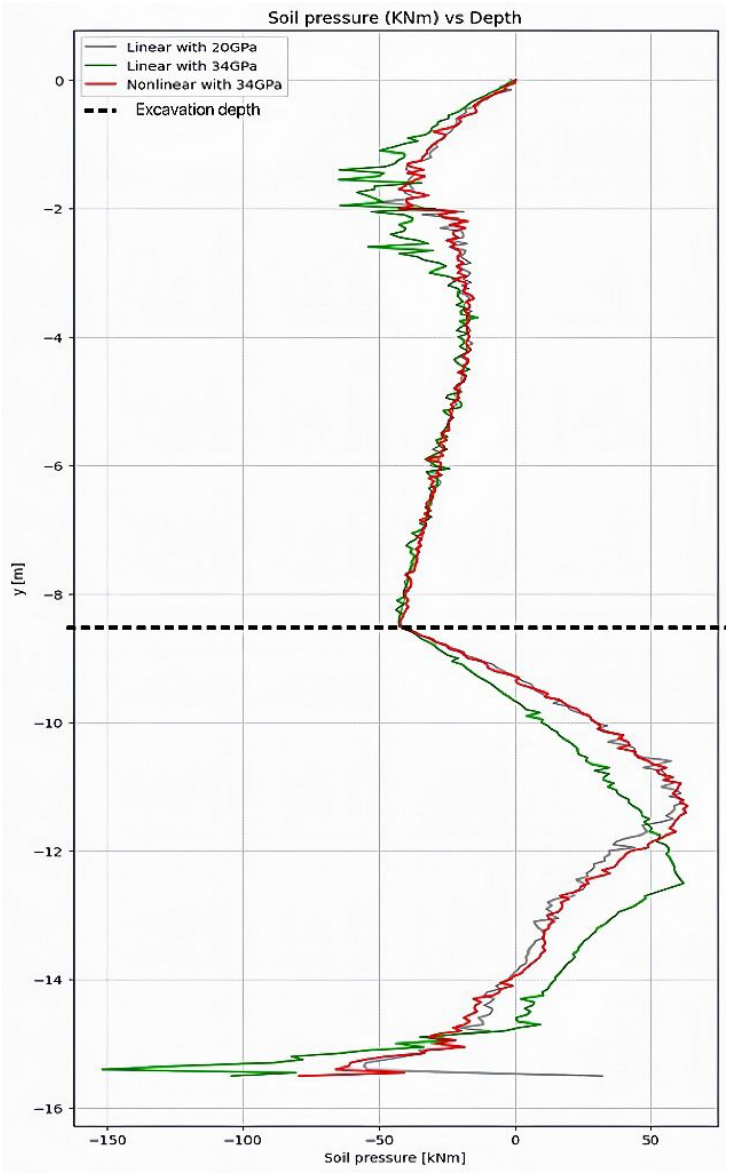

Figure 3.5.: Soil pressure for 3 analysis

3.4.2. Ground side soil pressure

In Figure 3.6, the green line represents the active soil pressure on the ground side, indicating the soil failure line when unloaded. It is evident that from -4m to -8.5m, the results from all three analyses overlap with the active pressure. This indicates that the soil in this zone has already transitioned to active pressure (soil already failure), moving with the wall as a flow. Therefore, that's also prove why in the total soil pressure result as Figure 3.5, from -4 to -8.5m, the three analyses results for soil pressure are overlapped.

3.4.3. Excavation side soil pressure

From -8.5m to -11m in Figure 3.7, the results from the three analyses show overlapping soil pressures, indicating that the soil in this zone is nearing failure and aligns with passive soil pressure. Except this zone, the soil is not failure for excavation side. However, the total soil pressure figure reveals differences in this excavation soil side failure zone because it accounts for both excavation-side and ground-side soil pressures. Since the ground-side soil has not failed, this contributes to the difference observed in the total soil pressure within this depth range.

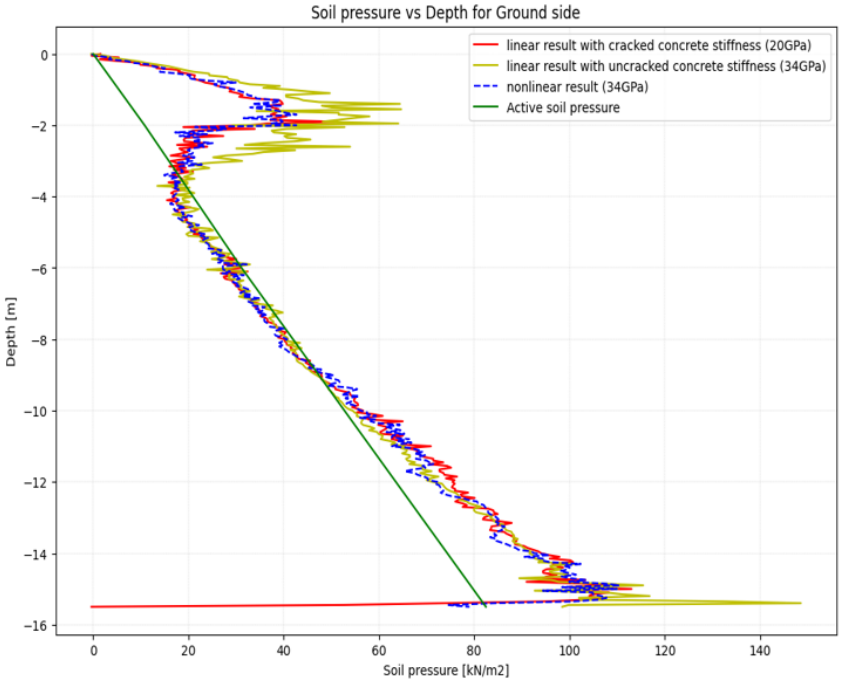

Figure 3.6.: Ground side soil pressure for 3 analysis

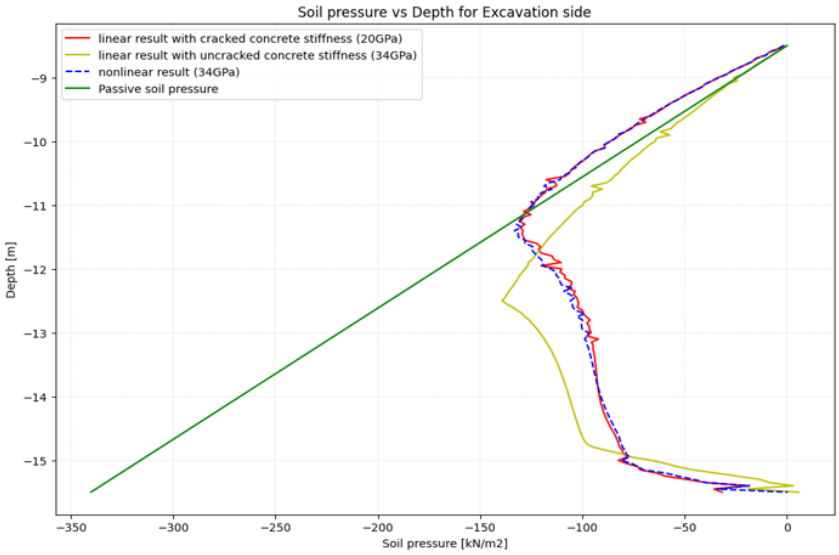

Figure 3.7.: Soil passive pressure for 3 analysis

Above all, the wall displacement, and soil pressure for analyses L20, L34, and NL could clearly explain the variations in bending moment distribution observed across the three analyses.

- **Above the excavation depth**:

The nonlinear concrete analysis shows the lowest peak bending moment among the three analyses, then the largest result is from the linear concrete analysis with original concrete stiffness. Above the excavation side, the soil lateral pressure only considers the ground side soil pressure.

The reason why there has the differences among three analyses above the excavation depth of D-wall bending moment distribution:

1. Soil pressures are the same:

For the bending moment distribution above the excavation depth, the peak bending moment occurs between -5 and -7.5 meters. In this region, the soil has already reached a failure state. As a result, soil pressures across the three analyses are consistent even with the different displacement, with the soil moving alongside the wall.

2. Concrete stiffness is the lowest for NL:

As discussed in Chapter 2, nonlinear concrete analysis can model cracking behavior, which **reduces concrete stiffness** in cracked zones.

In contrast, the two linear concrete analyses (L20 and L34) cannot adjust concrete stiffness in response to cracking, resulting in a uniform stiffness throughout, even in areas that would experience reduced stiffness in a cracked condition.

As shown in Figure 3.3, cracking occurs above the excavation depth. Consequently, the nonlinear concrete analysis results in a reduction of concrete stiffness mainly in this region of the diaphragm wall, resulting the lowest concrete stiffness in this region.

In conclusion, when cracking occurs under identical soil pressure conditions, the nonlinear concrete analysis shows the lowest effective concrete stiffness. This reduced stiffness results in greater wall displacement and reduces the peak bending moment of the diaphragm wall (D-wall) above the excavation depth. In practical terms, the reinforcement design based on the L20 bending moment shows a peak moment value just 11 kNm higher than the nonlinear analysis result. Given the minimal difference, any refinements to reinforced concrete design in this area would be limited.

- **Below the excavation depth**:

In contrast to the results above the excavation depth, below the excavation depth, the nonlinear concrete analysis indicates the highest peak bending moment. Conversely, the linear concrete analysis, using the original concrete stiffness, shows the lowest peak value in this region. Below the excavation depth, soil pressure results from both the ground side soil pressure and the lateral soil pressure exerted by the excavation side.

To explain the reason why happens the differences below the excavation depth of D-wall bending moment distribution:

1. Soil pressures are different:

As shown in Figure 3.4, the wall displacements of L20 and NL overlap, resulting in the same soil pressure.

For L34, the wall displacement is minimized, as discussed in Chapter 2. In loaded soil conditions, greater wall movement results in increased lateral pressure. However, the reduced wall displacement corresponds to a decrease in soil pressure compared to L20 and NL, resulting in the lowest peak bending moment below the excavation depth. In this area, the soil has not completely failed.

2. Concrete stiffness are different:

Firstly, since no cracking occurs in this zone, the nonlinear concrete analysis does not reduce the concrete stiffness. Since under the same soil pressure, the higher stiffness in the NL in this region compared to L20, its bending moment peak exceeds that of the L20.

In summary, below the excavation depth of the D-wall, the peak bending moment occurs outside the cracked zone. As a result, the concrete's stiffness for NL remains unchanged, retaining its original, non-cracked value.

With same wall displacement and soil pressure as in the L20, the NL—using the original, higher concrete stiffness—produces a higher peak bending moment in this zone.

On the excavation side, where the soil pressure is compressed, as Figure 2.3 shows the reduced movement of the wall leads to a decrease in the soil pressure on the wall. Consequently, the peak bending moment from the L34 is minimized, benefiting from that.

Below the excavation depth, the peak bending moment occurs on the ground side of the diaphragm wall (D-wall). Therefore, when comparing the NL results with the L20 bending moment results, it indicates that the L20 design for reinforced concrete does not provide a sufficient safety margin in this scenario.

From the variations in the bending moment distribution above and below the excavation depth, it is evident that there are two different mode of soil concrete interaction:

- **As the soil already failure, the soil pressure stay the active/passive soil pressure. And the D-wall happens crack in this soil failure zone, the nonlinear analysis produce the low stiffness in this zone, resulting the low bending moment distribution in the soil failure zone.**
- **As the soil not fail and is under compression, the less wall displacement leads to lower lateral soil pressure on the D-wall. This decrease in lateral pressure helps reduce the bending moment distribution in the compressed soil zone.**

The reason why the original stiffness concrete analysis produced the least D-wall displacement result below the excavation depth:

a. The D-wall with original linear stiffness is stiffer than in the other two analyses, resulting in less displacement overall. b. The wall displacement continuity requires that changes above the excavation depth impact the entire wall, ensuring consistent displacement throughout of whole wall.

3.5. Soil behavior result

The case study bending moment distribution examines two distinct soil conditions: a soil failure scenario and a soil compression scenario. To further analyze soil behavior under unloading conditions, specific soil elements are selected to closely study the critical points in bending moment distribution, as illustrated in Figure 3.8.

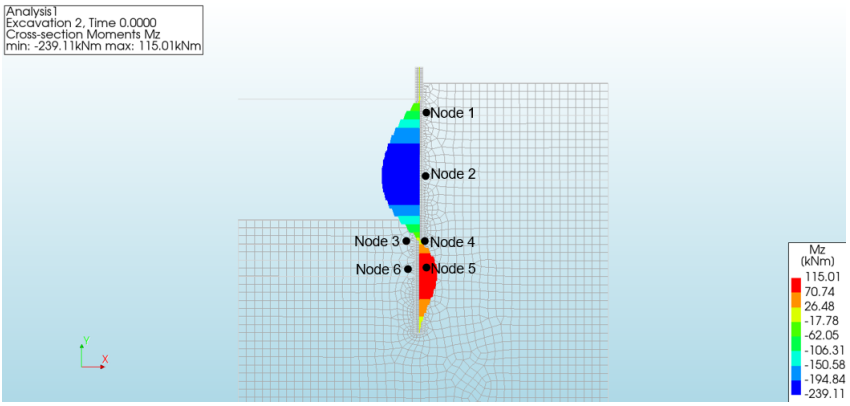

Figure 3.8.: Soil elements selection

The most critical point in soil element behavior is Node 5. The behavior of the other nodes is analyzed and presented in the Appendix B. Node 5's soil behavior is depicted in Figure 3.9, where the X-axis represents the horizontal displacement of the soil element and the Y-axis represents the horizontal soil pressure. This plot illustrates the soil's response throughout the entire construction process, from the beginning to the end of construction.

The results for Node 5 from the three analyses indicate that the soil element experiences an unloading scenario throughout the entire construction process. The black line represents the nonlinear concrete analysis, showing the largest soil displacement and the lowest horizontal pressure. In contrast, the green line, which corresponds to the linear concrete analysis with original stiffness, indicates the least soil movement and the highest soil pressure. These results confirm that, as shown in Figure 2.3, when the soil is unloaded and remains stable (not failing), increased soil movement leads to a decrease in lateral soil pressure.

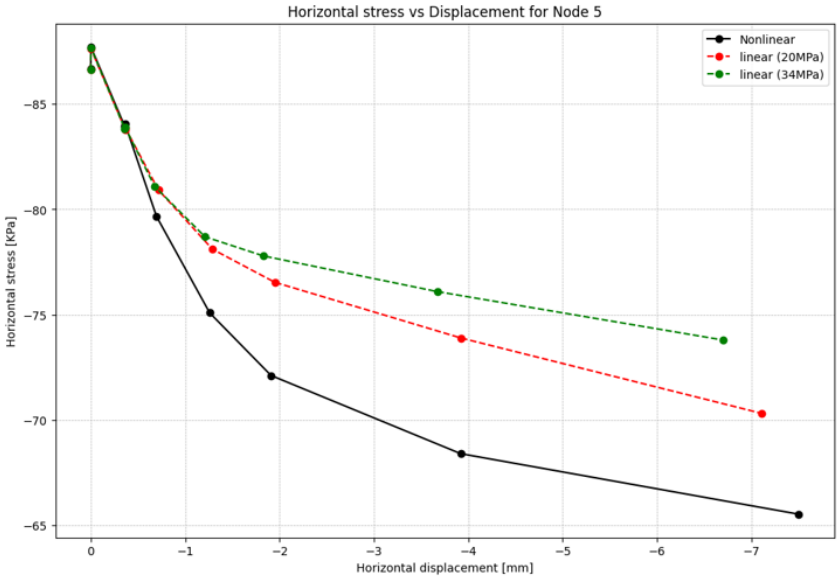

Figure 3.9.: Node 5 soil element behavior

In conclusion, Node 5 illustrates how soil behaves under unloading conditions, demonstrating soil-structure interaction as shown in Figure 2.3. This provides insight into a third soil condition:

- **As soil not fail and under unloading, the more wall displacement leads to lower lateral soil pressure on the D-wall. This decrease in lateral pressure helps reduce the bending moment distribution in the unloading soil zone.**

Since Node 6 is located at the same depth as Node 5, it exhibits a similar displacement value, as illustrated in Figure 3.10. The soil, being a continuous material, is influenced by its neighboring soil, resulting in slight variations in the displacement results. Positioned at the excavation side, Node 6 first experiences unloading due to excavation. Once the soil stabilizes, it undergoes compression as the wall deforms toward the excavation side.

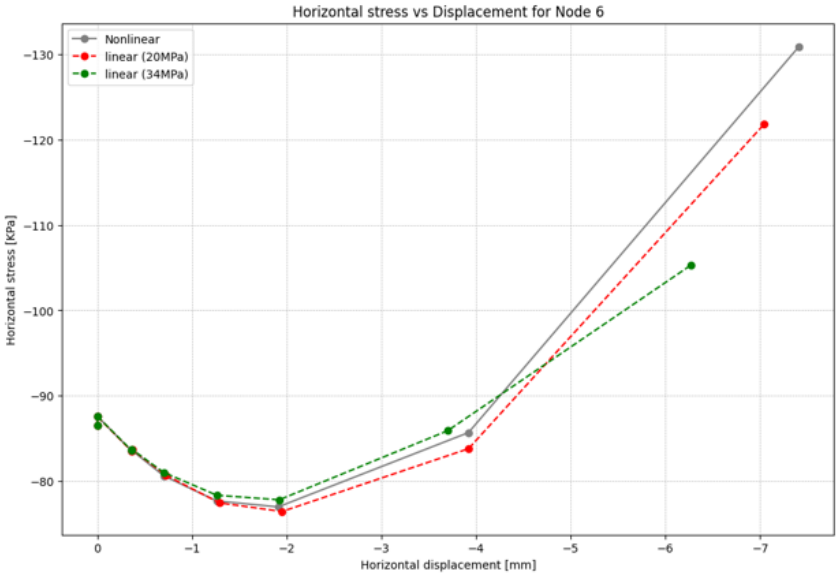

Figure 3.10.: Node 6 behavior

4. Practical case

After examining the soil-structure interaction mechanisms in the case study presented in Chapter 3, a discussion of practical applications will be conducted. Same as the case study, the three analyses are conducted to enable a comparison among them.

4.1. Bending moment result

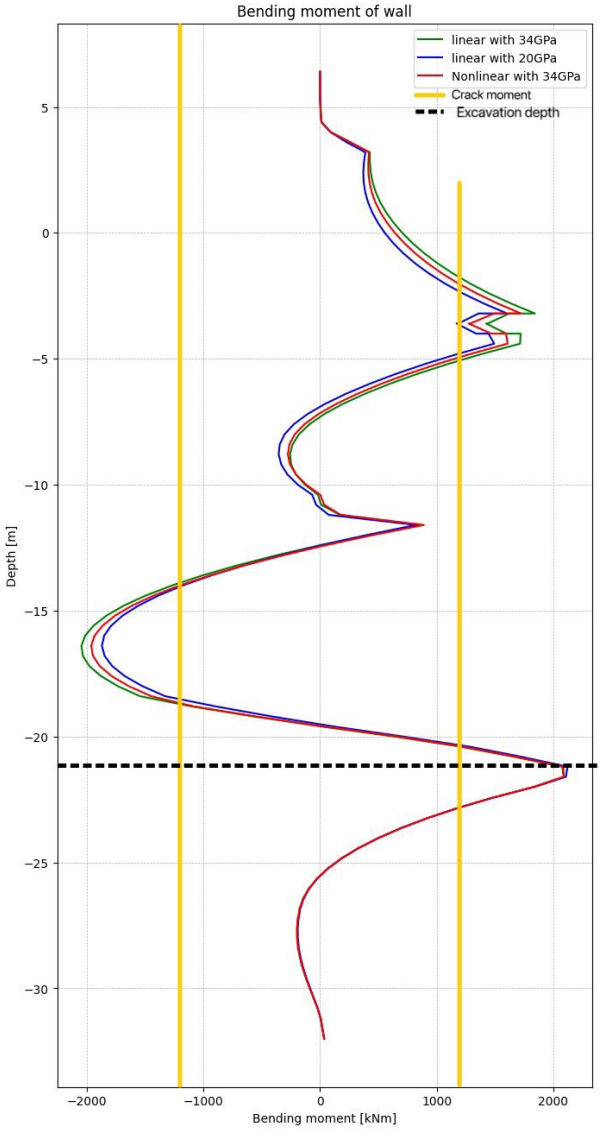

Figure 4.1.: Bending moment result for three analysis in practical model

1. **L34:** Soil nonlinear and concrete linear analysis with original concrete stiffness (Green line).
2. **NL:** Soil nonlinear and concrete nonlinear analysis with original concrete stiffness (Red line).
3. **L20:** Soil nonlinear and concrete linear analysis with reduced concrete stiffness (Blue line).

As shown in Figure 4.1, the blue dashed line represents the 20 GPa concrete linear analysis (L20), the red line represents the nonlinear concrete analysis (NL), and the green line represents the 34 GPa concrete linear analysis (L34). The yellow line represents the crack moment for the diaphragm wall in a practical scenario, indicating cracking on both the excavation and ground sides.

The bending moment results from the three analyses show that the NL, L20, and L34 results largely overlap at most locations. In the peak bending moment zones, L34 exhibits the largest values, followed by NL, with L20 showing the smallest values. However, the differences between them are minimal.

In practice, the three analyses show almost overlap because the diaphragm wall reinforcement is overly dense and heavy. This excessive reinforcement causes the diaphragm wall to behave like an extremely stiff bar, resulting in similar responses for the L20, L34, and NL models.

In pratical case, the L20 analysis provides a relatively accurate approach for reinforced concrete design in practical cases.

4.2. Soil pressure result

As shown in Figures 4.2 and 4.3, the soil pressure results from the three analyses are presented for both the ground and tunnel sides. On the ground side, the soil pressure results overlap at most locations, showing no significant differences between the analyses. This suggests that the soil above the excavation depth is close to failure, as indicated by the similarity in soil pressure. This contrasts with the case study, where notable variations in soil pressure were observed.

On the tunnel side, the peak pressure is primarily caused by the grouted soil, which exhibits a significantly higher pressure in that zone. The results of the three analyses show consistent overlap for the tunnel side, reflecting the similarity in behavior across all three methods in this grouted zone.

The overlap in soil pressure on both the tunnel and ground sides indicates a corresponding overlap in the bending moments across the three analyses.

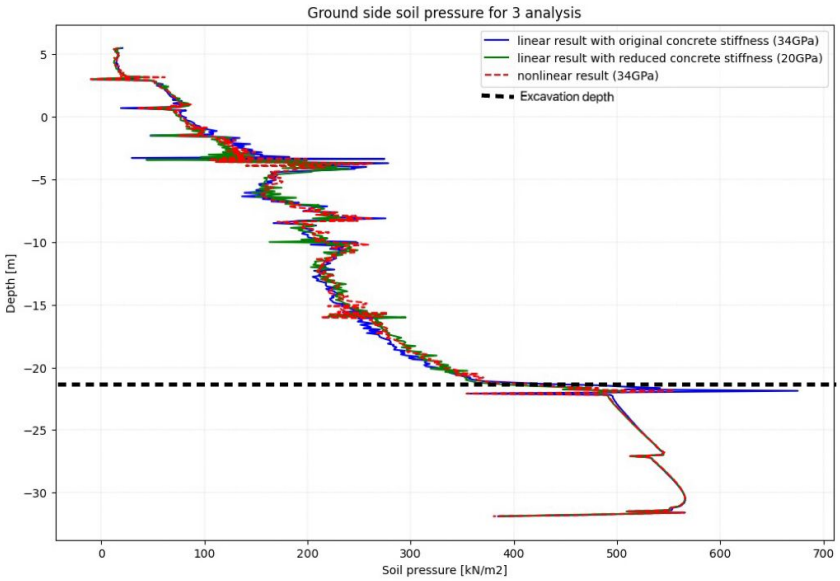

Figure 4.2.: Soil pressure for 3 analysis in ground side

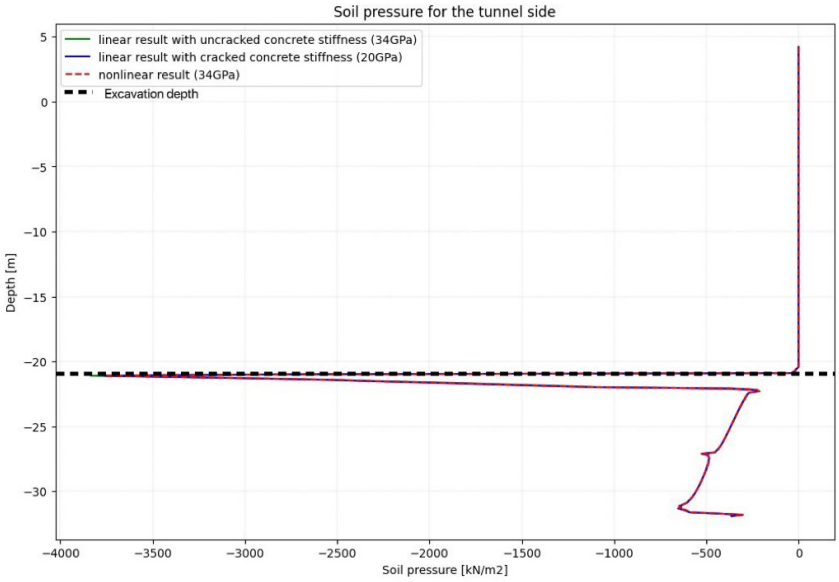

Figure 4.3.: Soil pressure for 3 analysis in tunnel side

4.3. Wall displacement result

Figure 4.4 presents the D-wall displacement results for the three analyses. Above the excavation depth, the L34 and NL result almost overlap for wall displacement above the excavation depth, with the largest displacement in L20. However, the differences between the three analyses are minimal, with a maximum displacement variation of only 2.1 mm, indicating a limited impact on soil-structure interaction. Below the excavation depth, the three analyses results are overlap.

To explain the overlapping bending moment distribution of the three analyses above the excavation depth, consider the following assumptions:

- In both the L34 and NL analyses, wall displacements are nearly overlap overall, leading to closely soil pressure and result in overlapped bending moment distribution.

- In the L20 analysis, wall displacement is at its maximum, and concrete stiffness is lower. If soil failure does not occur, the resulting soil pressure should be significantly lower than in L34.

However, as shown in Figure 4.2 the ground side soil pressure, the results from the three analyses almost overlap. This suggests that the soil is near failure above the excavation depth, where soil pressure remains stable even with additional movement. Thus, in this practical case, the soil above the excavation is close to a failure scenario, offering limited opportunities for optimizing reinforced concrete design through soil-structure interaction.

Below the excavation depth, the three analyzes wall displacement overlap, then cause the soil pressure are same for the three analyzes.

Below the excavation depth, extending to -25 m, wall displacements are significantly smaller than those above the excavation. The wall displacement is directed to the right due to high soil pressure from the soil grout in this region, which pushes the wall in that direction. Consequently, the diaphragm wall may allow more deformation below the excavation depth.

However, as wall displacement increases, the soil pressure below the excavation also rises, leading to higher soil loads. In practical cases, the complexity of these conditions means that nonlinear concrete analysis and soil-structure interaction offer limited benefits for design refinement.

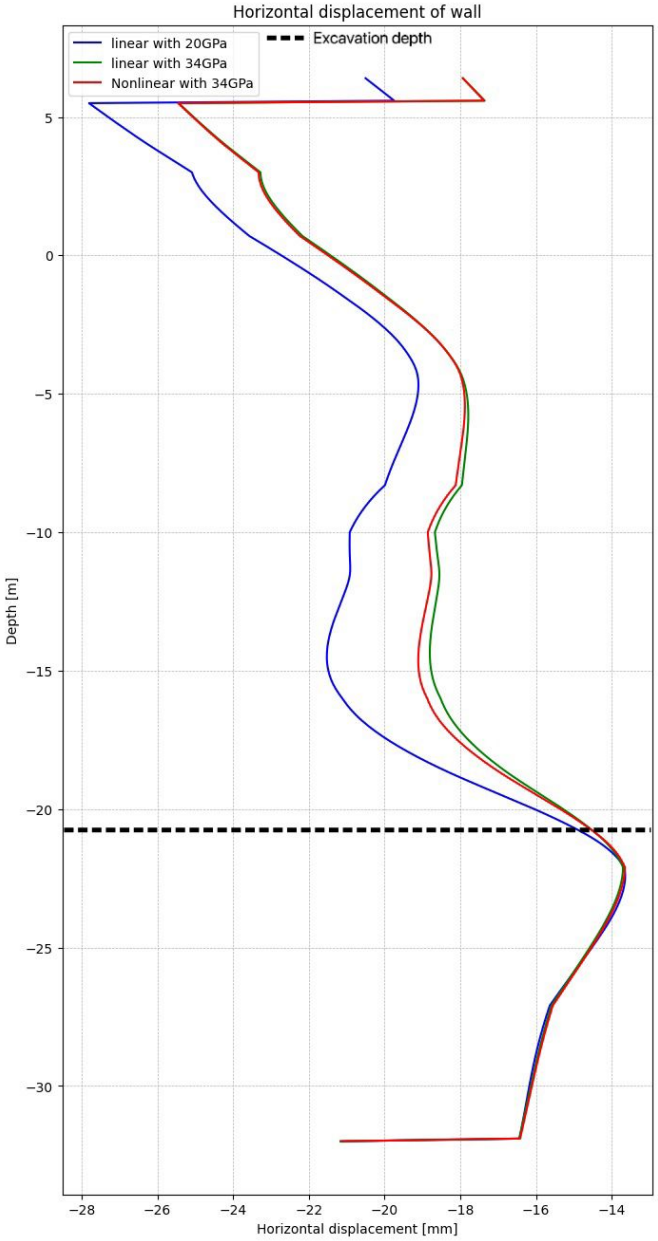

Figure 4.4.: Wall displacement for 3 analysis in practical case

Above the excavation depth, the soil is nearly at failure; thus, further wall movement does not significantly change soil pressure. Below the excavation depth, increased wall displacement leads to a rise in soil pressure, which in turn raises the bending moment, increasing reinforcement requirements.

In conclusion, combining nonlinear concrete analysis with soil-structure interaction provides limited benefit in this practical case due to the extreme soil conditions.

5. Conclusion

5.1. Case study

For the case study, there are three scenario for soil structure interaction for Diaphragm wall:

1) **As the soil already failure, the soil pressure stay the active/passive soil pressure. And the D-wall happens crack in this soil failure zone, the nonlinear analysis produce the low stiffness in this zone, resulting the low bending moment distribution in the soil failure zone.**

2)**As the soil not fail and is under compression, the less wall displacement leads to lower lateral soil pressure on the D-wall. This decrease in lateral pressure helps reduce the bending moment distribution in the compressed soil zone.**

3)**As soil not fail and under unloading, the more wall displacement leads to lower lateral soil pressure on the D-wall. This decrease in lateral pressure helps reduce the bending moment distribution in the unloading soil zone.**

The three scenarios—soil failure, soil loading, and soil unloading—each uniquely impact soil-structure interaction, resulting in distinct effects on the bending moment distribution. These variations necessitate potential refinements in reinforced concrete design to account for the specific bending behaviors associated with each soil condition.

5.2. Practical case

In the practical case verified in the case study—particularly the scenario involving soil failure and concrete cracking—only limited improvement in bending moment distribution is observed. The high density of reinforcement results in minimal cracking, leaving little room for further refinement, especially given that the soil has already failed.

Additionally, in practical applications, another scenario can often be observed:

4)**As the soil has already failed, the soil pressure remains at active or passive levels. The diaphragm wall (D-wall) remains uncracked, so the nonlinear concrete analysis retains its original, higher stiffness rather than a reduced stiffness. However, this increased stiffness does not benefit the bending moment distribution; instead, it results in higher soil pressures, potentially increasing reinforcement requirements.**

In this research, four types of soil-structure interactions were observed in the diaphragm wall (D-wall), each corresponding to different conditions of soil and concrete.

To emphasize the conditions of the concrete and soil, this research identifies four distinct states:

- **Soil fail, concrete crack:** Nonlinear concrete analysis helps reduce the bending moment distribution in soil failure zone, as the nonlinear concrete stiffness decrease.
- **Soil not fail (under compression), concrete not crack:** Nonlinear concrete analysis could not help reduce the bending moment distribution, as the nonlinear concrete stiffness stay original stiffness.
- **Soil not fail (unloading), concrete not crack:** Nonlinear concrete analysis helps reduce the bending moment distribution, as the concrete wall moves more and reduce the soil pressure load on the wall.

- **Soil fail, concrete not crack:** Nonlinear concrete analysis could not help reduce the bending moment distribution, as as the nonlinear concrete stiffness stay original stiffness.

5.3. Potential refinement

Given that nonlinear analysis and soil-structure interaction offer limited advantages for reinforced concrete design in practical cases, the reinforcement design approach should be reconsideration.

In the reinforced concrete design outlined in Appendix C, the bending moment is currently based on the maximum value across both sides of the wall. An alternative approach to optimize reinforcement would be to design based on the maximum bending moment in divided segments, adjusting the longitudinal reinforcement accordingly in each segment. This method could reduce overall reinforcement requirements by tailoring reinforcement levels more precisely to the bending moment distribution along the wall.

A. Appendix:Methodology for FEM

A.1. Finite Element Method Programs

This section provides a concise summary of various programs identified as capable of modelling the soil-structure interaction, and non-linear analysis for soil and concrete. The assessment of these programs is based on an analysis of their websites and user manuals, as well as a review of literature where these programs are referenced. The advantages and disadvantages of each program will be analyzed. The criteria used for comparison found within the documents are:

- Concrete Models: What kind of concrete models are available in different FEM program?
- Soil Models: What kind of soil models are available in different FEM program?
- Interface: How to model the different interface?
- Element: What kind of element available in different FEM program?
- Result: What kind of plots will be provided by program?
- Analyses: Which analyses available in different FEM program?
- Design approach: What design criteria available in FEM program?

1. DIANA:
In Diana, there are many constitutive model available. For soil model, it not only has linear model for elastic perfectly plastic model, but also has non-linear model for different type of soil such as Cam-clay model (CC model), Modified Cam-clay model (MCC model), and Hardening soil model(HS model). For concrete, it also has non-linear model which can be used for concrete simulation, which models can model non-linear behavior and incorporate cracking. For example, the Multi-directional fixed crack model, and Total strain crack models. Furthermore, Diana have plenty of different elements such as shell, solid element, and reinforcements elements as well as crack tip elements, embedded reinforcement model, bond-slip model, which could be used for modelling the reinforcement D-wall. Also for the interaction between the D-wall and soil, the non-linear interface element can be adopted. To display the D-wall internal force result, different plot types are available such as stain-stress distribution, displacements. To achieving the non-linear analysis of D-wall, the Diana could provide structural nonlinear analysis and stability analysis. The user's manual is very clear and well-organized, there are a lot of tutorials for users to learn how to use DIANA. The capability to design in accordance with the Eurocode is a significant feature of DIANA.

2. PLAXIS:
PLAXIS is well known for geotechnical modelling. It provides various soil model such as soft soil model, soft soil creep model, besides the CC, MCC and HS model. Moreover, it can choose different behavior of soil like drained, undrained behavior. However, PLAXIS does not have non-linear model for modelling concrete behavior. And for reinforcement there is no model for non-linear modelling for reinforcement but it does have linear models that can be applied with concrete reinforcement propertied. For modelling the joints of different panels, the PLAXIS can model the joints as hinges in 2D version. Additionally, to model the interface between the D-wall and the soil, a joint element could be used, characterized by its specific friction angle and adhesion properties. To present the result of calculation, different kinds of plots are available for displaying like stress-strain distribution plot, bending moment plot as well as the deflection plot.In terms of the element available in PLAXIS, the high-order volume element are provided by PLAXIS. For modelling the D-wall, the plate and beam elements could be used. The Phi-c reduction analysis could used for computing the safety factor, and sensitivity analysis also available in PLAXIS. The manual for PLAXIS is well-explained and comprehensive, and a lot of tutorial about PLAXIS is available in website.

	DIANA	PLAXIS
Concrete models	++	+/-
Soil models	+	++
Interface	+	+
Element	++	+
Result	++	++
Analyses	++	+
Design approach	+	+

Table A.1.: Summary of the FEM programs and their scores based on criteria

- Conclusion

As the table 1 shows, the scores for DIANA and PLAXIS are given based on the criteria. The comparison between the Diana and Plaxis, it is clearly to present that the Diana is more suitable for modelling the Diaphragm wall behaviour with consideration of non-linear behavior and soil-structural interaction. Plaxis has more advanced soil models than Diana, however, it does not have non-linear model for concrete. This study focus on the optimization the design of reinforcement, therefore, the non-linear behavior for concrete should be emphasized.

A.2. Analysis

After determining that the FEM software should use DIANA, the subsequent step involves following the procedure to build the FEM model in DIANA.

The primary objective is to explore how the diaphragm wall interacts with the surrounding soil, with a particular focus on the D-wall behavior. This led to the decision to employ **Structural Analysis** as the preferred method for this research. In addition, the construction process includes drainage stages. As a result, changes in the water table should be calculated, necessitating the inclusion of a **Groundwater Flow** analysis in the overall assessment.

A.3. Dimension

When simplify the modeling of diaphragm walls under stress and strain, a 2D approach can be adopted instead of complex 3D modeling, to save time and resources. Advanced 2D numerical modeling can effectively capture the dynamic of soil-structure interaction by considering the excavation step, pore water pressure change, and the influence of proximity of tunnels to diaphragm walls.
There are several different ways could be adopted for analysis D-wall:

Plane strain: This analysis assumes the material extends infinitely perpendicular to the analyzed plane, so the deformation in that direction is zero, which is ideal analysis for long structures such as dams and walls.

Generalize plane strain: Generalized plane strain analysis in Diana is an advanced form of plane strain that allows for some out-of-plane deformation. This is particularly useful in cases where the structure, when the structure is elongated but not infinitely long and might experience uniform loads or displacements at its ends, thus requiring the consideration of such effects in the analysis.

Two-dimensional: In Diana software, 2D analysis typically involves elements confined to a plane, without considering stresses or deformations extending beyond that plane, making it suitable for analyzing thin structures.

Conclusion: Given the assumption that the diaphragm wall extends infinitely long and this is no out-of-plane stresses or strain, the **plane strain** is the most appropriate dimensional setting.

A.4. Model size

Given the dimensions of the Diaphragm wall, ranging from +6.4m to -32m, and the need for precise modeling of both the structure and soil behavior, the model's dimensions should be **at least 30m (width) by 60m (length)** to ensure accuracy.

A.5. Mesh type and order

In Diana, there are two different setting for mesh types:

Hexa/Quad: Hexa/Quad elements refer to hexahedral (3D) and quadrilateral (2D) shapes, typically used in finite element analysis for their ability to accurately model straight and curved boundaries with less elements.

Tetra/Triangle: Tetra elements are tetrahedral (3D) and triangular (2D), which is preferable for dealing with complex geometries because of flexibility but may require more elements to achieve the same level of accuracy as Hexa/Quad elements.

Conclusion: To achieve the accuracy requirement, the **Hexa/Quad** is selected as the mesh type in this modeling.

For mesh order, linear elements use first-order interpolation for faster computations but may offer less precision. In contrast, quadratic elements employ second-order interpolation, enhancing accuracy at the expense of increased computational time. Given the importance of precision in research, quadratic elements are often preferred for modeling despite the higher computational demand.

A.6. Geometry

The original model is shown in Figure A.1 . The three purple walls are diaphragm walls, and the middle blue wall is a construction wall that only exists during construction. This construction wall does not significantly influence the whole system. Therefore, it is unnecessary to take into account the behavior of the construction wall between D-wall 2 and D-wall 4. The entire system can be symmetrical, with the middle of D-wall 2 serving as the axis of symmetry as the FigureA.2 shows. The simplified symmetrical model is on the right side of the whole system.

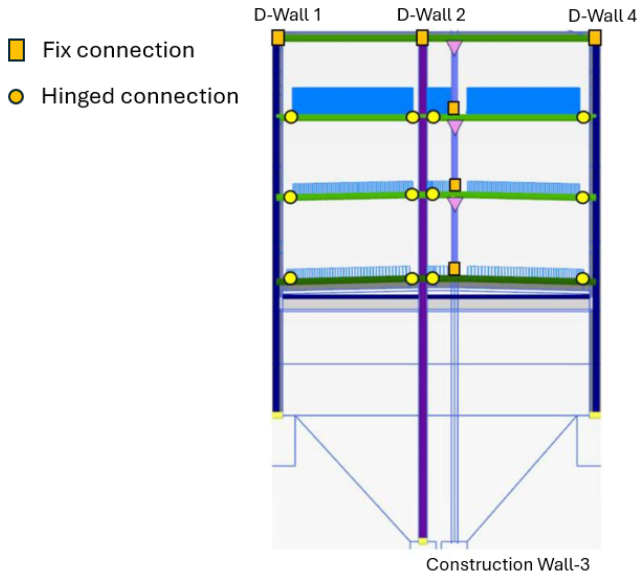

Figure A.1.: Original geometry of D-wall section

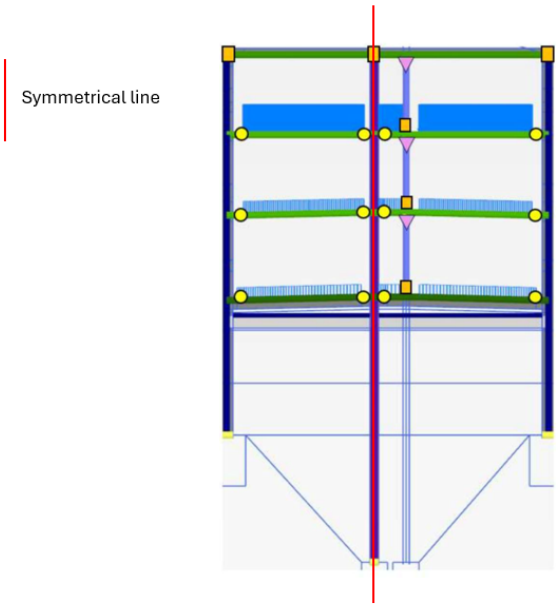

Figure A.2.: The symmetrical line location

After determining the model, based on the cross-sectional D-wall underground soil layer, draw the simplified symmetrical model as shown in the figure.

Table A.2.: Soil Layers and Properties

Soil layer	Soil type	Top of the layer (m)
1	Backfill sand	5.5
2	Quaternary clay	3.2
3	Lillo1, sand	0.7
4	Lillo2, sand	-1.5
5	Kattendijk, sand	-3.65
6	Berchem1, sand	-8.3
7	Berchem3, sand	-10
8	Berchem4, sand	-15.5
9	Boom clay	-22.1

Table A.3.: Ground water table

Ground water level	Location
Ultimate Limit state(ULS)	+4.75m
Serviceability Limit state(SLS)	+4.25m

A.7. Element

- Diaphragm wall concrete:

There are several options for modelling the D-wall concrete in Diana. Normally, there are two different way to model the D-wall concrete element:

Table A.4.: Wall Dimensions and Thicknesses

Floor	Top of the wall (m)	Bottom of the wall (m)	Thickness (mm)
Top Roof	4.2	3.3	1200
Floor -1	-3.2	-4.2	900
Floor -2	-10.65	-11.55	900
Bottom floor	-18.6	-20.1	1500

Table A.5.: Strut Specifications

Strut	Level (m)	Spacing (m)	Diameter (mm)	Thickness (mm)	Preload (kN)
Strut 0	4.2	3.4	1120	20	0
Strut -1	-0.46	3.4	1120	20	2500
Strut -2	-7.14	3.4	1120	20	5000
Strut -3	-15.5	3.4	1120	20	7500

Infinite shell: Infinite shells, designed as line-shaped plane strain elements with a small thickness relative to their length, are ideal for modeling structures presumed to be infinitely long, like diaphragm walls. This approach effectively simulates the diaphragm wall as an infinitely long structure with a specific thickness and a flat shape, making the infinite shell model a suitable choice for such scenarios.

Volume: The volume element is 3-D element with three spatial dimensions(length, width and height). In order to analyse the D-wall complex behavior, the 3-D element could be a choice for accurate analysis, and to provide detailed interaction with surrounding soil and other structure. In addition, to effectively illustrate the thickness of a Diaphragm wall and incorporate the reinforcement cage within the concrete, employing volume elements can enhance the visualization of the reinforced-concrete wall structure. Unlike the infinite shell, which is represented as a line in the XY plane, volume elements offer a more comprehensive representation by showing the wall with a certain thickness in the XY plane, making them a superior choice for comprehensive visualization.

Conclusion: In order to visualize the modeling better and make more convenience of operation when combine with the soil surrounding the D-wall. The volume element is selected to model the concrete diaphragm wall. For post-processing analysis result, the composed line elements are used for calculating the local forces and bending moments in a model's cross-section by integrating primary stresses or internal forces over the plane normal to a defined line. The composed line elements including all regular elements and embedded reinforcements, do not influence the stiffness or material properties.

- Diaphragm wall reinforcement:

There are several options for modeling the reinforcement element as discuss in Chapter 2. The Embedded reinforcement, Bond-slip reinforcement, and Shear reinforcement. Embedded Reinforcement elements are used for view of reinforcement behavior. For stirrups, both embedded bar or grid could be used. Shear Reinforcement is the method for capturing shear forces in the model. Additionally, the reinforcement element should combine with the line component.

- Soil:

For modeling soil behavior, Diana often employs the **Plane strain** element to simulate soil behavior. This approach is typical when the structure's length greatly exceeds its height and depth as the soil length should be large to guarantee the accuracy of modelling . Initially, the choice of dimension is a 2D plane strain, thus, a 3D stress analysis is not considered in this context.

- Floor

Because the floor is directly connected to the D-wall, both of which have a specific thickness, a **Volume element** (identical to the D-wall element) is selected for modeling the floor's behavior. Using a different element for the floor could result in inconsistent stiffness distribution and a distorted mesh transition from the D-wall to the floor, potentially leading to numerical instability. This impacts the accuracy and convergence of the solution

- Struts

Due to the fact that struts are designed to transfer axial tension or compression loads and do not support bending moments or shear forces, truss elements are the preferred choice for simulating this behavior in strut analysis. **Truss elements** are ideally suited for this, as they are specifically designed to handle only axial forces.

- Soil-structure interaction (Soil - Diaphragm wall interface)

Considering the soil-structure interaction, between the soil and D-wall there should be a connection to simulate the frictional interaction between the soil and the structure. The **interface element** which is particularly useful for simulating the nonlinear behavior that occurs at the interface, such as sliding and potential separation under extreme load conditions.

- Floor-diaphragm wall connection (Interface between D-wall and floor)

Due to the differing connection methods between floors, the top floor is fixedly connected to the D-wall, while the other floors are hinged connected.

In a hinged connection, the rotation allowed between the floor and the D-wall, so an tension cut-off **interface element** should be established between the floor and the D-wall to model the hinged interaction. Therefore, the tension cut-off interface element is adpoted to simulate the hinged connection. Another way to model the hinged connection is the geometry method to simulate the hinged behavior.

In contrast, with a fixed connection, the behavior of the interaction between the D-wall and the floor should be modeled by **unifying** these two components into a single system. This ensures a smooth transfer of forces and moments across the connection.

- Conclusion

Table A.6.: Element using in the modelling

Object	Element selection
Diaphragm wall concrete	Volume elements
Diaphragm wall reinforcement	Embedded Reinforcement elements
Soil	Plane strain elements
Floor	Volume elements
Struts	Truss elements
Soil-structure interaction	Interface elements
Floor-Diaphragm wall interaction	Interface (Hinged) Unite (Fixed)

A.8. Material property

- Linear concrete model:

The concrete adopted for this research is **C35/45**. For the linear analysis for concrete, the linear-elastic model adopted in this model. The parameter required for this model:

- Non-linear concrete model:

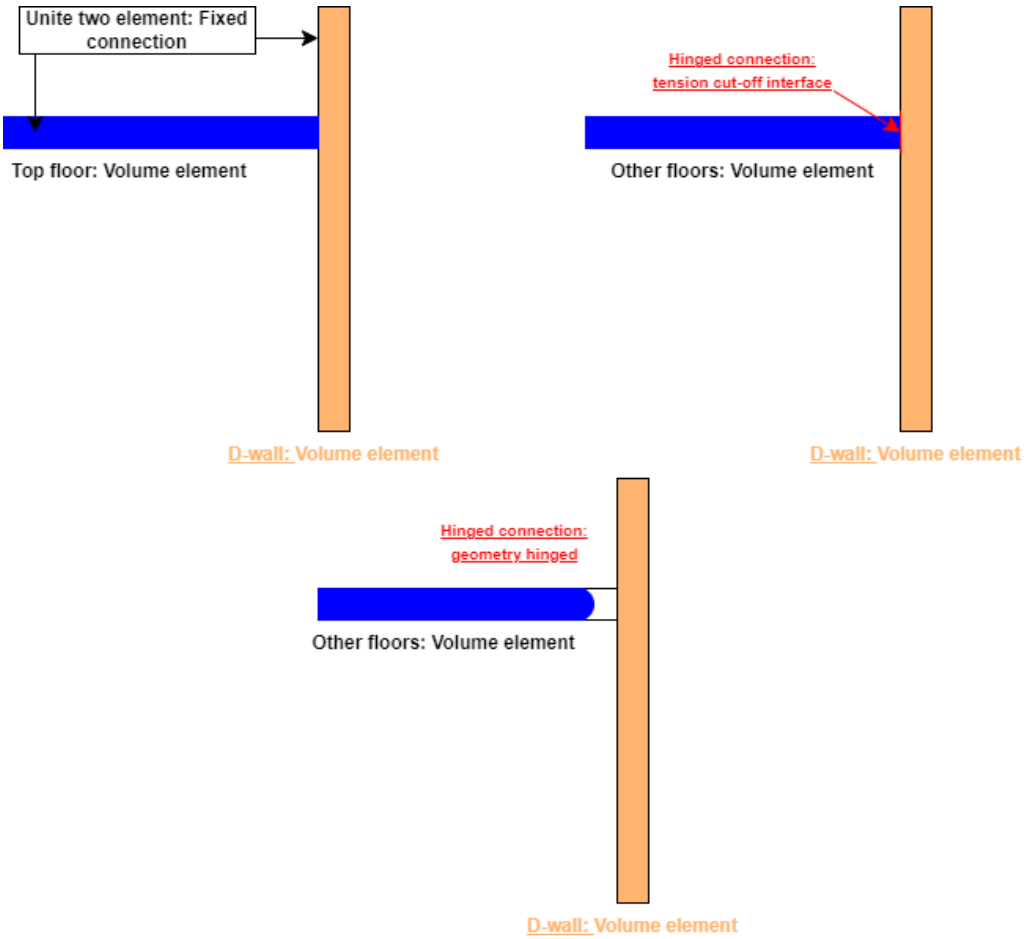

Figure A.3.: Fixed and Hinged connection

Table A.7.: Linear elastic parameter for C35/45 concrete

Young's modulus E_{cm}	34077 (MPa)
Unit weight γ	25.0 kN/m^3
Unit density ρ	2500 kg/m^3
Poisson's ratio v	0.2 (Uncracked concrete)

As discussed in Chapter 2. There are several non-linear model could be used for modeling the concrete behavior. The Total Strain-Based Rotating Crack Model is selected for simulate behavior of reinforcement concrete. The rotating crack model, which has garnered positive experiences in comparison to the fixed crack model, typically predicts a lower limit failure load. This is primarily because the rotating model is less susceptible to the adverse effects of spurious stress-locking. On the other hand, the fixed crack model always result in considerably higher failure loads Research and Technical Development, 2022. For modeling the tensile behavior of reinforced-concrete, adopting the exponential-type softening diagrams as suggested by Research and Technical Development is advantageous. This approach leads to more localized cracking, which helps in avoiding the formation of large areas of diffuse cracking. Due to incomplete knowledge about the actual properties of materials, the variability in reinforced concrete materials is excessively large. To minimize the introduction of further errors, it may be leave some non-critical (not required) parameters (residual tensile strength) unspecified. The compressive behavior of concrete is complex, as evidenced by its experimental response under uniaxial compression, which demonstrates a softening relationship post-peak strength. A favored modeling approach utilizes the compressive fracture energy, denoted as G_c. This model accurately captures the softening behavior by determining the crushing band width, h_{eq}. It employs a parabolic stress-strain diagram that includes a softening branch, based on the value of the compressive fracture energy.

Table A.8.: Non-linear elastic parameter for C35/45 concrete

Linear material property	**Young's modulus** E_{cm}	34077 (MPa)
	Unit weight γ	25.0 kN/m^3
	Unit density ρ	2500 kg/m^3
	Poisson's ratio v	0.2 (Uncracked concrete)
Total strain based crack model	**Crack orientation**	Rotating
Tensile behavior	**Tensile curve**	Exponential
	Tensile strength $f_{ctk,0.05}$	2.21 MPa
	Mode-I tensile fracture energy	1.782MN/m
Compressive behavior	**Compressive curve**	Parabolic
	Compressive strength f_{cd}	23.33 MPa
	Compressive fracture energy	29.233 MN/m

- Soil model:

There are different soil model discussed in Chapter 2. However Teo and Wong, 2012. As discussed in Chapter 2, the Hardening soil model is selected to model soil behavior.

Table A.9.: Soil Layers and Properties

No.	**Soil Type**	**Top of the layer (mNAP)**	γ_{unsat} **(kN/m^3)**	γ_{sat} **(kN/m^3)**	ϕ^* **(°)**	ψ^* **(°)**
1	Backfill sand	5.50	18.0	20.0	32.5	0
2	Quaternary clay	3.00	18.5	18.5	22	0
3	Quaternary clay	0.70	18.5	18.5	20	0
4	Lillo 1, sand	0.70	16.5	19.4	30	2
5	Lillo 2, sand	-1.50	16.5	19.4	35	5
6	Kattendijk, sand	-3.50	17.0	19.9	35	5
7	Kattendijk, sand	-8.30	17.0	19.9	35	5
8	Berchem 1, sand	-8.30	16.8	19.7	30	2.5
9	Berchem 3, sand	-10.00	16.8	19.7	32.5	3.5
10	Berchem 4, sand	-16.00	16.8	19.7	30.5	3
11	Boom Clay	-22.10	20.0	20.0	26	0
12	Boom Clay	-27.10	20.0	20.0	26	0
13	Boom Clay	-50.00	20.0	20.0	26	0

- Reinforcement model:

As Chapter 2 discussed, the Embedded reinforcement model should be applied, both embedded bar or grids can be used. As table A.11 shows.

Table A.11.: Reinforcement Properties

Material property	**Linear elasticity**	Young's modulus E_{cm} = 210000 (MPa)
Model selection	**Embedded reinforcement**	Embedded/Grid bar

- Strut model:

The linear material property is adopted to strut model, because the steel is used for the strut material. Therefore, based on the Eurocode 2, the parameter for the strut material model shows in table A.12.

Table A.10.: Hardening Soil Model Properties of Soil Layers

No. soil layer	**POP (kN/m^2)**	**OCR**	$K_{0;NC}$	v_{ur}	$K_{0;mid}$	**m**	**k (m/s)**
1	10	1	0.463	0.20	0.55	0.50	1.16×10^{-4}
2	10	1	0.625	0.20	0.71	1.00	1.16×10^{-7}
3	10	1	0.658	0.20	0.73	1.00	1.16×10^{-7}
4	10	1	0.500	0.20	0.54	0.50	1.16×10^{-4}
5	10	1	0.426	0.20	0.45	0.50	1.16×10^{-4}
6	10	1	0.426	0.20	0.44	0.50	1.16×10^{-4}
7	10	1	0.426	0.20	0.44	0.50	1.16×10^{-4}
8	10	1	0.500	0.20	0.51	0.50	1.16×10^{-4}
9	10	1	0.463	0.20	0.47	0.50	1.16×10^{-4}
10	10	1	0.492	0.20	0.50	0.50	1.16×10^{-4}
11	750	1	0.562	0.30	0.89	0.00	5.00×10^{-9}
12	750	1	0.562	0.30	0.79	0.70	1.50×10^{-10}
13	750	1	0.562	0.30	0.70		
No. soil layer	**Ref (kN/m^2)**	**m***	**c**	E_{Oed} **(MN/m^2)**	E_{50}**(MN/m^2)**	E_{ur}**(MN/m^2)**	G_0**(MN/m^2)**
1	100	0.50	0	12	12	49	62
2	100	0.80	0	5	4.8	14	17
3	100	0.80	2	4	4	16	20
4	100	0.50	2	11	11	44	55
5	100	0.50	0	16	16	63	79
6	100	0.50	0	84	84	337	421
7	100	0.50	0	91	91	363	454
8	100	0.50	0	31	31	123	154
9	100	0.50	0	44	44	175	219
10	100	0.50	0	33	33	134	167
11			40/20	7	10	44	106
12			40/20	10	15	65	120
13			40/20				

Table A.12.: Material Properties for Structural Steel

Material property	**Value**
Unit Weight γ	78.5 kN/m^3
Young's Modulus E	210000 MPa
Poisson's Ratio ν	0.3

- Floor model:

The model used for floor material model is the same as the **D-wall linear concrete model**.

- Soil-structure interaction model:

For the soil-structure interaction between soil and the diaphragm wall, an elastic-plastic model is used to describe the behavior of interfaces for the modelling of soil-structure interaction. The Coulomb friction model is used to distinguish between elastic behavior, where small displacement can occur within the interface, and plastic interface behavior when permanent slip may occur. For the interface to remain elastic the shear stress τ given by:

$|\tau| < \sigma tan\phi_i + c_i$

where $|\tau| = \sqrt{\tau_{S1}^2 + \tau_{S1}^2}$.

Where τ_{s1} and τ_{s2} are shear stress in the two (perpendicular) shear directions and σ_n is the effective normal stress.

For plastic behavior τ is given by:

$|\tau| = \sigma tan\phi_i + c_i$

The value of R_{inter} can be adopted, R_{inter} is the strength reduction factor. In general. for real soil-structure interaction the interface is weaker and more flexible than the associated soil layer, which means that the value of R_{inter} should be less than 1. In the Plaxis Manual, the R_{inter} suggested to be $2/3$ if this absence of detailed information. In this research, taking the consideration of bentonite used before the construction of D-wall. The R_{inter} value should set lower than $2/3$, considering the lubricating effect of bentonite.

Therefore, to set the $R_{inter} = 0.5$

When adopt the R_{inter} in the interface element:

$c_i = R_{inter} c_{soil}$

$tan\phi_i = R_{inter} tan\phi <= tan\phi_{soil}$

$\psi_i = 0$ for $R_{inter} < 1$, otherwise $\psi = \psi_{soil}$.

Furthermore, the normal and shear stiffness values at the interface should be set high to prevent slippage between the soil and concrete. Such high stiffness levels are crucial for enabling the interface element to effectively transfer loads between the concrete and soil, ensuring structural integrity and performance.

Therefore, the parameters used in soil-structure interaction should be shown in the Table A.13.

Table A.13.: Properties of Various interface parameters

Type of Soil	Normal Stiffness (KPa/m)	Shear Stiffness (KPa/m)	Cohesion (KPa)	Friction Angle (°)
Backfill sand	1.00×10^9	2000	0	17.67
Quaternary clay	1.00×10^9	2000	1	11.42
Quaternary clay	1.00×10^9	2000	0.5	10.31
Lillo 1, sand	1.00×10^9	2000	0	16.1
Lillo 2, sand	1.00×10^9	2000	0	19.3
Kattendijk, sand	1.00×10^9	2000	0	19.3
Berchem 1, sand	1.00×10^9	2000	0	16.1
Berchem 3, sand	1.00×10^9	2000	0	17.67
Berchem 4, sand	1.00×10^9	2000	0	16.1
Boom Clay	1.00×10^9	2000	10	13.7

- Floor-Diaphragm wall interaction model:

In the modeling of the floor-diaphragm wall hinged connection interface, the interaction between the concrete elements is non-linear behavior. There are two options to model the floor-diaphragm wall interaction: tension cut-off interface, the geometry way.

For the tension cut-off interface way to model the hinged connection, to satisfy the non-linear requirements, Coulomb friction model is effectively used here to simulate this interaction. For the parameter setting, to ensure the stability of the floor and preventing it from collapsing, it is crucial to consider the cohesion at the interface. While the actual cohesion between concrete surfaces can vary, in modeling, it is often set high to ensure adequate safety against sliding, which is only for the tension cut-off interface way to simulate the hinged connection. For the choice of a friction angle for the tension cut-off interface way to model the hinged connection which is based on empirical values observed in practice. The friction angle between concrete surfaces is typically reported to be between 29 to 35 degreesEng-Tips

Forums, 2023. Therefore, selecting an average value, such as 30 degrees, provides a reasonable balance between accuracy and simplicity for engineering purposes. Regarding the dilatancy angle, it is generally assumed that it is zero for concrete in both design conditions. The reason for using the tension cut-off in the interface model is particularly important because it allows the model to ignore tensile stresses, which concrete is poor at resisting. By setting the tension cut-off to zero, the model effectively prevents any tensile transmission across the interface, ensuring that the analysis focuses on compression and shear, which are more critical for the structural integrity of such interfaces. This setup also facilitates the rotation between the interfaces, which is characteristic of hinged connections, without the complications of consideration of tensile stress. Using a tension cut-off interface to simulate the hinged connection is a highly effective method.

To model the concrete interaction geometrically, the floor slab is depicted as being inserted into the wall's console. To create a more realistic hinged connection, cohesion and friction should be minimized, allowing the floor slab to rotate freely without transferring any bending moment to the D-wall. Additionally, sharp corners at the console should be avoided to prevent high stress concentrations. To address this, the sharp part of the console should be cut, and a disconnect interface applied between the console and the slab, ensuring the separation of these two elements, as shown in FigureA.4.

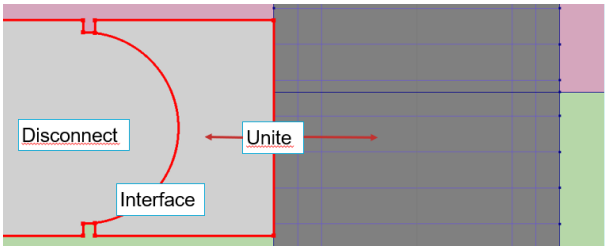

Figure A.4.: The geometry way of hinged connection

Compared to the tension cut-off interface to model the hinged connection, the geometry way to simulate is closer to realistic of hinged connection mechanism. However, the geometry way requires more time to build the model.

In conclusion, the parameter for the two different way to model the hinged connection shows as Table A.14 and Table A.15. In Chapter **??**, there is a discussion regarding the selection between these two approaches

Table A.14.: Properties of tension cut-off interface for Hinged Connection

Type	Normal Stiffness (MPa/m)	Shear Stiffness (MPa/m)	Cohesion (kPa)	Friction Angle (°)	Dilatancy Angle (°)	Tension Cut-off (kPa)
Concrete Interface	1000000	2	5e+09	30	0	0

Table A.15.: Properties of Geometry-Based Hinged Connection

Connection Type	Normal Stiffness (MPa/m)	Shear Stiffness (MPa/m)	Cohesion (kPa)	Friction Angle (°)	Dilatancy Angle (°)
Concrete Interface	1000000	2	1	1	0

A.9. Construction stage

As table A.16 shows, there are 21 stages for the total construction phase. And there are 3 phases related to drainage.

Table A.16.: Construction Stages

No.	Construction Phase
1	Preparation (Before apply D-wall)
2	Pre-load
3	Apply D-wall
4	Excavate to 2.8m TAW + **Drainage** to 2.8 m TAW
5	Soil improvement (grout soil)
6	Installation strut 0
7	**Drainage** to be determined above Boom clay +2m
8	Excavate to -0.6 m TAW
9	Installation strut 1
10	Excavate to -4.2 m TAW
11	Apply floor -1
12	Remove strut 0
13	Apply roof
14	Strut -1 remove
15	Excavate to -8.3 m TAW
16	Install strut 2 with VSP
17	Floor -2 apply
18	Excavate to -11.8 m TAW
19	Remove strut 2
20	Excavation to -16.5 m TAW
21	Installation stamp 3 with VSP
22	Final excavation stratum to -20.43 m TAW and **drainage** to -20.7 m TAW
23	Apply bottom floor
24	Remove strut 3

A.10. Load condition

For the different floors, there are different load condition during the construction phase and final construction. The detailed condition shows in Table A.17.

Table A.17.: Load values for different floors during construction and final phases

Floor	Construction phase Permanent [kN/m^2]	Construction phase Variable* [kN/m^2]	Final phase Permanent [kN/m^2]	Final phase Variable* [kN/m^2]
Mezzanine floor -1	n/a	5.5	5.5	12.0
Mezzanine floor -2	n/a	5.5	6.0	24.0
Bottom floor	n/a	5.0	6.0	20.0

B. Appendix: Case study model

B.1. Mesh and load step influence

Before determining the results of a linear analysis, it is essential to verify the mesh quality and load step configuration. Variations in mesh size and the number of load steps can significantly impact the stability and accuracy of the finite element model. To ensure the stability and correctness of the model, different mesh sizes and load step types should be tested. The optimal mesh size and load step should then be selected based on this evaluation to conduct a reliable analysis.

- Mesh size influence

For the mesh size test, to keep the load steps same for construction stage, and to change the mesh size for D-wall from 0.5m to 0.05m. For this analysis, the bending moment is the critical result that requires the most attention. Therefore, sensitivity analysis should be conducted to assess the influence of mesh size and load steps, specifically focusing on their impact on the bending moment results. As Figure B.1 shows, for the finite element model of one size, get a three-time analysis result and calculate the variance for the mesh group of one size, to compare the variance for different mesh sizes. And for the different mesh size, to get the average value from the results, and to check the overall stability of the result.

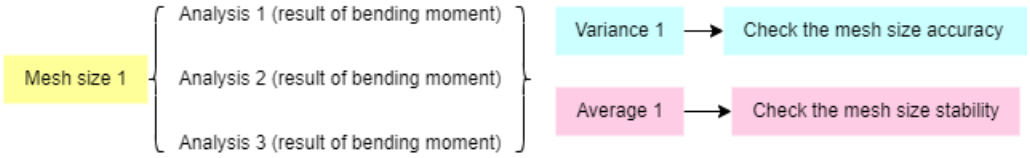

Figure B.1.: Mesh size analysis

There are 6 different mesh sizes chosen to test, as Table B.1 shows. And the load step adaptation for the construction stage is: preparation (1 step), apply D-wall (1 step), excavate to -2m (10 steps), installation strut 1 (steps), excavation to -5m (10 steps).

Table B.1.: Construction Stages for case study

No.	Mesh size for D-wall
1	0.5m
2	0.4m
3	0.3m
4	0.2m
5	0.1m
6	0.05m

Considering both the maximum bending moment change of the results, it was observed that the average value at 0.4m is significantly lower compared to the overall results, while the average value at 0.1m remains relatively stable. Therefore, the mesh size of **0.1m** is selected as the final mesh size.

- Load step influence

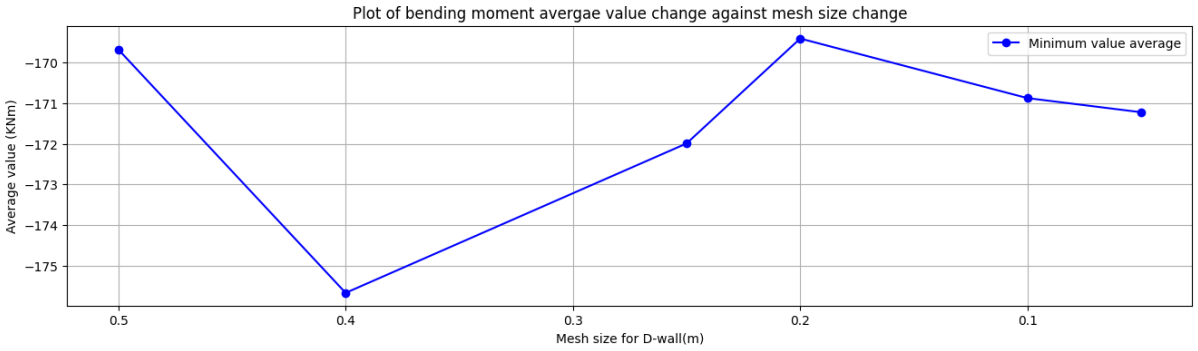

Figure B.2.: Mesh size influence for average value of bending moment

Similarly as the mesh size sensitivity analysis, the load step is varied from 2 to 20 while keeping the mesh size constant, with the goal of identifying the most suitable load step for this finite element model. As with the mesh size analysis, the bending moment result is used as the basis for the analysis. Following the same procedure as in the mesh size analysis, as shown in Figure B.3, the final load step is selected by comparing the mean values and variances of the results.

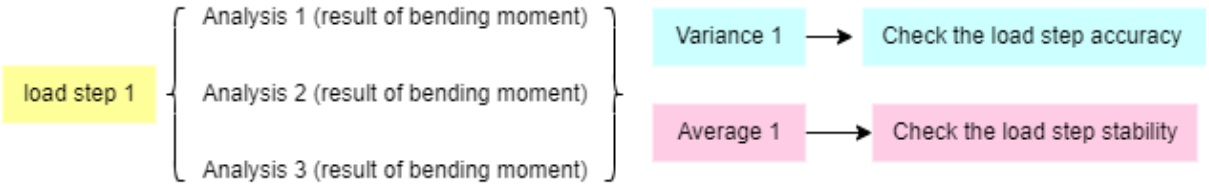

Figure B.3.: Load step influence analysis

Table B.2.: Different load step for the load step analysis

Load step type	Preparation	Apply D-wall	Excavation to -2.0m	Installation strut 1	Excavation to -7.5m
1	1	1	2	2	2
2	1	1	5	5	5
3	1	1	7	7	7
4	1	1	8	8	8
5	1	1	9	9	9
6	1	1	10	10	10
7	1	1	20	20	20

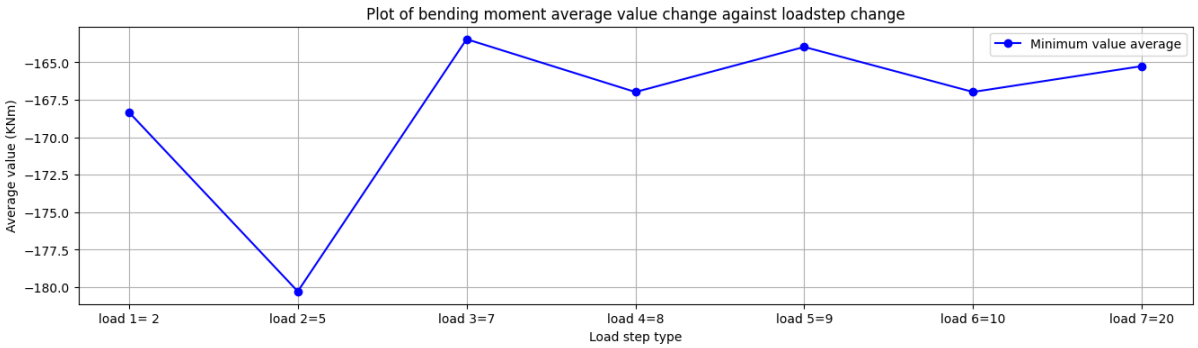

Figure B.4.: Average value change against load step change

Based on Figure B.4 the average value change, load types 4 and 7 both stay in the stable range. However, considering the computation time and resources, the **load type 4** is selected to be the final load step.

- Iteration times

As shown in Figure **??**, considering the stability of the results, the number of iterations was set to 50. This choice ensures that the average value stabilizes and the variance of the results is relatively low compared to other iteration counts.

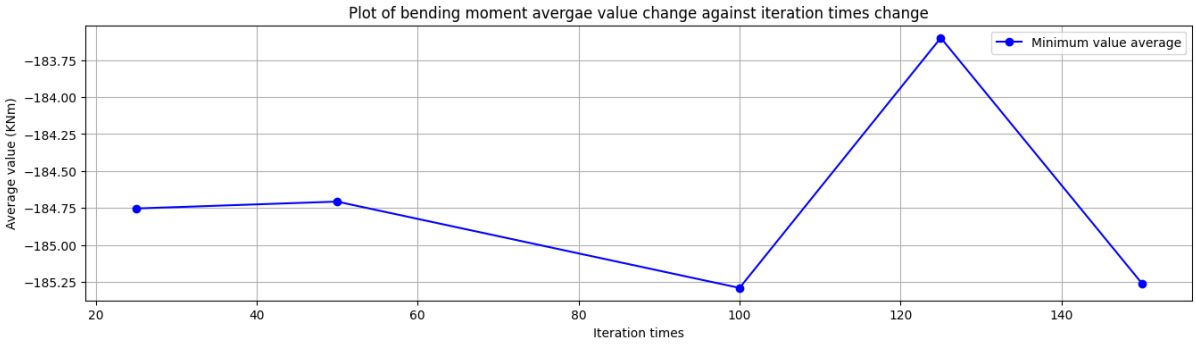

Figure B.5.: Average value change against iteration numbers change

Therefore, before starting the analysis of the linear analysis, the following setting is determined:

Table B.3.: The analysis setting

Mesh size for D-wall	0.1m
Load step for analysis	Load type 4
Iteration times	50

B.2. Soil non-linear wall linear analysis

After determining the load step and the mesh size for the analysis, the results are examined for phase displacement, shear force, normal force, and bending moment.

B.2.1. Phase displacement

- Apply the D-wall

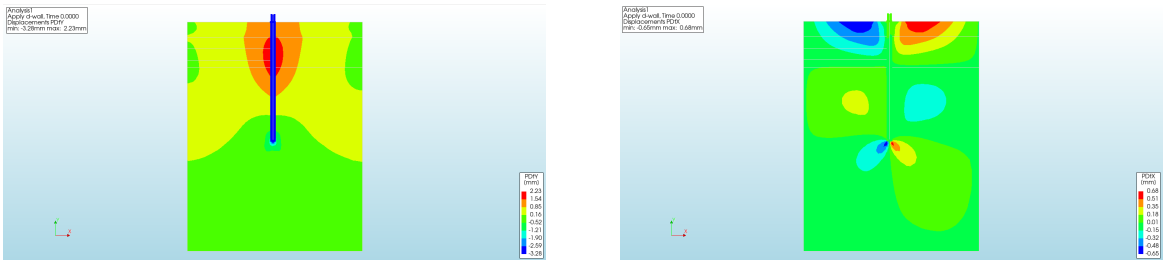

(a) Apply the D-wall displacement for Y direction

(b) Apply the D-wall displacement for X direction

Figure B.6.: Apply the d-wall phased displacement

As Figure B.6 shows, the direction Y is downwards -3.23mm due to the insertion of the D-wall, and the surrounding soil upwards 2.22mm. And the X direction is almost stable.

- Excavation to -2.0m

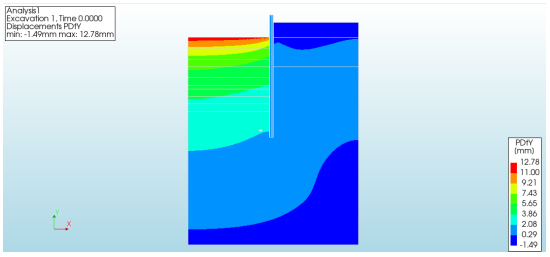

(a) Excavation to -2.0m displacement for Y direction

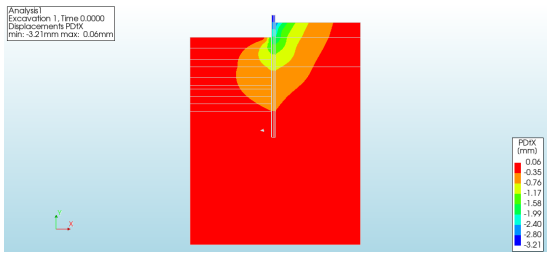

(b) Excavation to -2.0m displacement for X direction

Figure B.7.: Excavation to -0.2m phased displacement

In the construction stage of excavating to -2m, the Y direction moves upward 12.78mm, and the main displacement of the X direction is the wall move left side 6.41mm due to the swollen soil as shown in Figure B.7.

- Installation strut

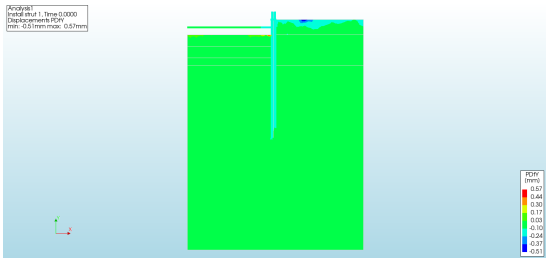

(a) Installation strut displacement for Y direction

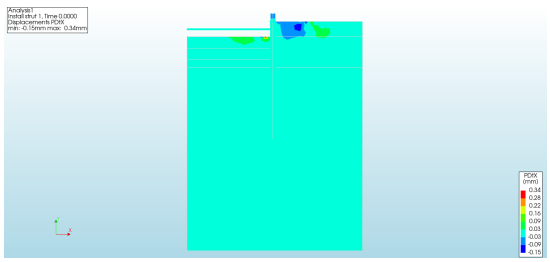

(b) Installation strut displacement for X direction

Figure B.8.: Installation strut phased displacement

Because the installation of the strut does not have a large impact on the entire system, the weight of the strut is light, shown in Figure B.8, the displacement of X and Y direction is not larger than 1mm.

- Excavation to -8.5m

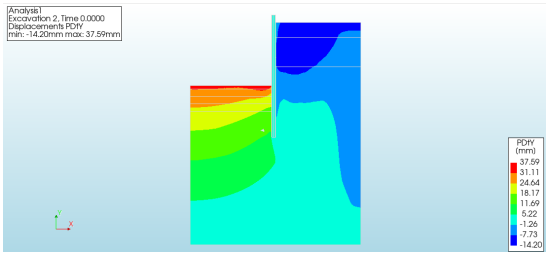

(a) Excavation to -8.5m displacement for Y direction

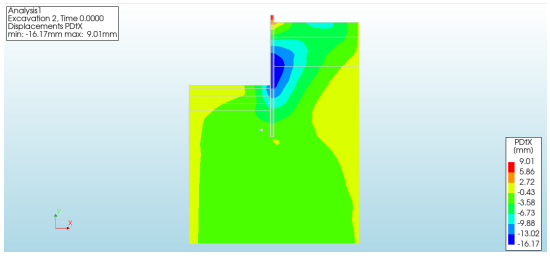

(b) Excavation to -8.5m displacement for X direction

Figure B.9.: Excavation to -8.5m phased displacement

As Figure B.9 shows, excavation to -8.5m, soil moves 37.59mm upwards at the excavation side and the ground side soil move downwards -14.20mm, and the X direction of the middle of the wall is inclining to the left side of 16.17mm.

B.2.2. Normal force

After examining all phased displacement of the analysis, the normal force, shear force and bending moment result of last construction step is selected for the next stage reinforcement design.

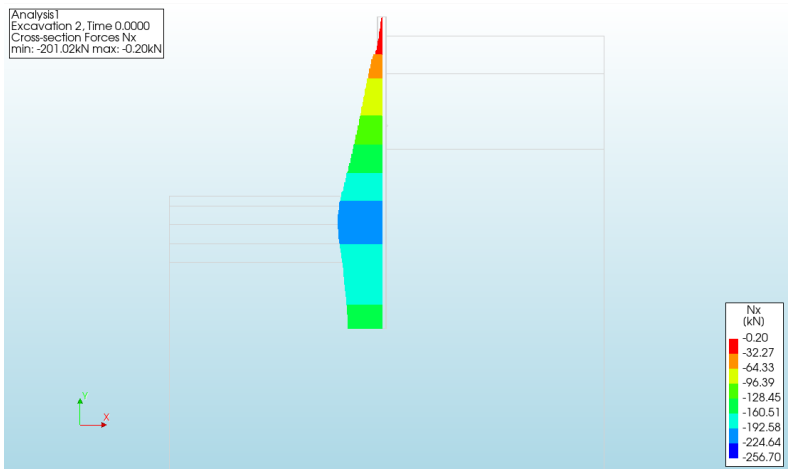

Figure B.10.: Normal force result for last construction stage

As shows in Figure B.10, the normal force is increasing from -0.2KN to -201.02KN (the maximum normal force), because of the soil pressure.

B.2.3. Shear force

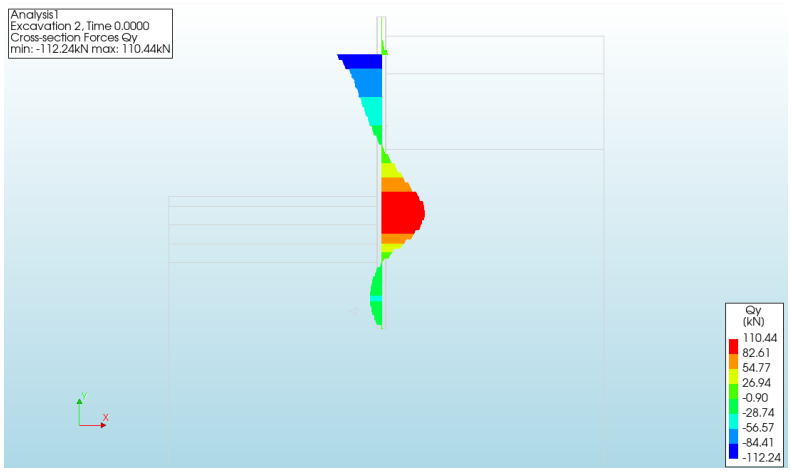

Figure B.11.: Shear force result for last construction stage

The shear force distribution on the D-wall, as illustrated in Figure B.11, exhibits the expected behavior under excavation loading conditions. Notably, there is a significant concentration of shear force near the strut, reaching a value of -112.24 kN. Additionally, a second peak is observed just below the final excavation surface, with a shear force value of 110.44 kN.

B.2.4. Bending moment

Figure B.12 illustrates that above the excavation surface the wall bending moment first peak with the value of -256.58 KNm. Below the excavation suface this is another bending moment peak with the value of 92.84 KNm. At the base, the bending moment is small with the value close to zero, indicating that the wall is sufficiently strong and stable after the construction process.

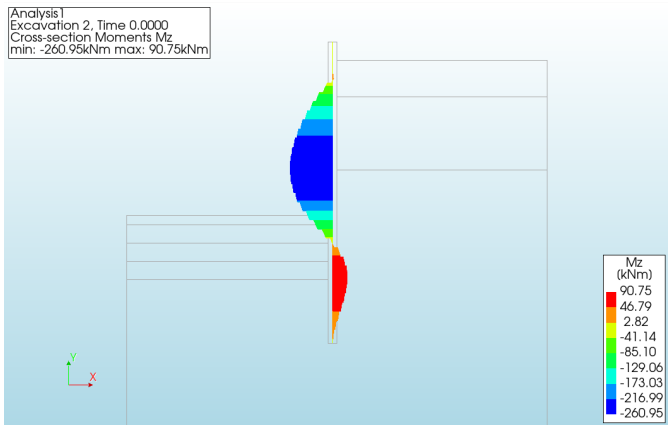

Figure B.12.: Bending moment result for last construction stage

B.3. Reinforcement Design

B.3.1. Design approach

- Design load for Ulitimate limit state

Based on Eurocode 7, the three design approach for geotechnical analysis could be used in Ultimate limit state design. And according to the , the Design approach 3 is commonly used in the Netherlands, which mentioned in Chapter 2. And the DA 3: ($A1^*$ or $A2^+$) "+" M2 "+" R3
$A1^*$: on structural actions. $A2^+$: on geotechnical action.
In this design only the structural actions safety factors is applied as Table B.4. The factor of soil parameter and partial resistance factors are not taken into account in this design.

Table B.4.: Partial factors on actions (A1)

Action		**A1**
Permanent	Unfavorable	$\gamma_G = 1.35$
	favorable	$\gamma_G = 1.0$
Variable	Unfavorable	$\gamma_G = 1.5$
	favorable	$\gamma_G = 1.0$

Therefore, the design bending moment and the shear force are multiplied by $\gamma_G = 1.35$, and the design normal safety factor is $\gamma_G = 1.0$The design bending moment is shown as Figure B.13, the blue line shows the simplified bending moment. And the green line shows the DA3 bending moment, the maximum value of design bending moment is 125 KNm, and the minimum bending moment is -350 KNm.

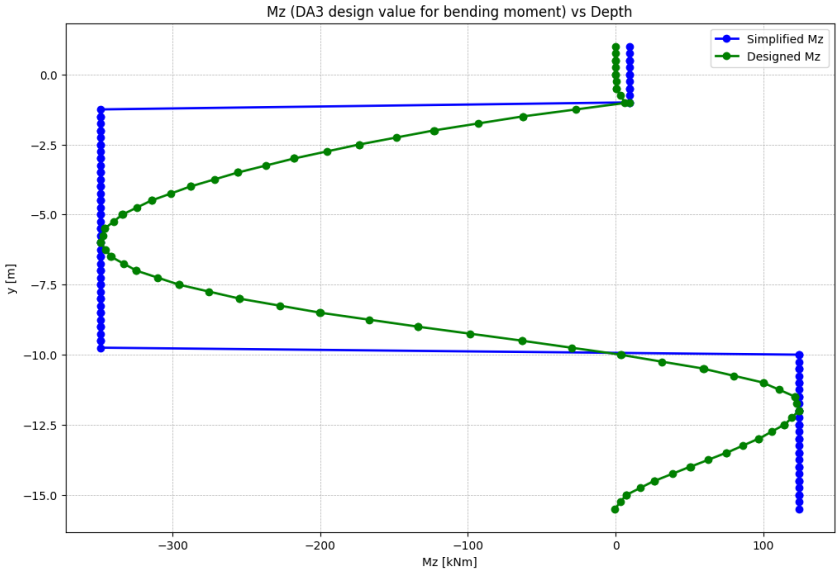

Figure B.13.: Design bending moment for case study

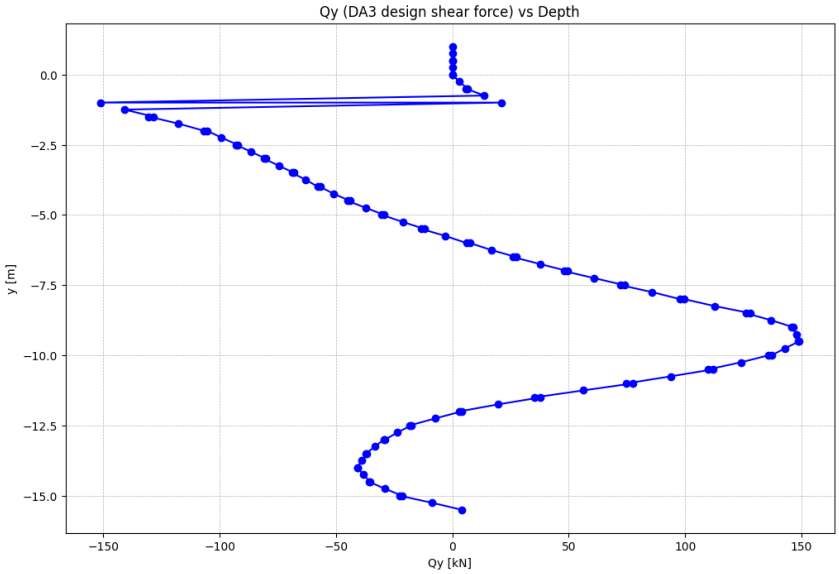

Figure B.14.: Design shear force for case study

The design approach value for shear force shows in Figure B.14. The maximum value is 149 KN, and minimum value for shear force is -152 KN. The normal force stays the same as before because it is unfavorable.

- Design load for Serviceability limit state:

The safety factor for the Serviceability limit state is 1.0. Therefore, the original external force is applied for the SLS design.

- Safety philosophy For linear analysis:

For the linear analysis, the design load discussed as above. For the concrete parameter in linear analysis, the partial factor method is employed. According to Eurocode 2, the following steps are applied in the **ULS design**.

◦ Concrete type: C35/45
◦ In this scenario, there is no water present, therefore, according to the Eurocode 2 Table 4.1, the Exposure classes should be **XC1**: concrete is permanently dry.
◦ Minimum applied cover $c_{min} = 40mm$.
◦ Coefficient taking account of long term effects and loading effects on the compressive strength of concrete (for bending): $\alpha_{cc} = 1$
◦ Concrete partial material safety factor: $\gamma_c = 1.5$
◦ Reinforcement steel partial material safety factor: $\gamma_s = 1.15$
◦ The design longitudinal reinforcement area should larger than $A_{s,min}$.
◦ The ULS bending moment resistance M_{Rd} of reinforcement should bigger than M_{Ed} (the design bending moment).

For the **SLS design**, For the SLS design, the following guidelines from Eurocode 2 should be applied to the serviceability limit state check:

◦ All the partial factor for SLS is 1.0.
◦ Because the exposure classes should be **XC1**: concrete is dry. And the allowance maximum crack width allowance $w_{max} = 0.4mm$ based on the Table 7.1N Eurocode 2.

- Safety philosophy for non-linear analysis:

For the non-linear analysis ultimate limit state check (**ULS**), the Global Resistance Factor is recommended by RTD-1016 and Eurocode 2 for non-linear analysis, which is mention in Chapter 2.
For the **SLS check** of the concrete, based on the RTD-1016:
In case of bending cracks opening w shall be calculated as: $w = S_{r,max} * \overline{\epsilon_s}$.
Where ϵ_s is the average strain value of the longitudinal reinforcement in the cracked zone.
$S_{r,max}$ is the maximum crack spacing.

B.3.2. Ultimate limit state and serviceability limit state design

Based on the last stage of construction, a reinforcement design is performed. As discussion above, the Ultimate limit state and Service limit state should be checked, the design and check are all based on Eurocode 2.

Table B.5.: D-wall first design for case study

D-wall Design	
Thickness	**0.5m**
Concrete type	**C35/45**
Reinforcement design	
Minimum required coverage C_{min}	**45mm**
Applied coverage C_{nom}	**50mm**
Excavation side reinforcement	**@20(150mm)**
Ground side reinforcement	**@20(315mm)**

- Ultimate limit state check

First, to check the reinforcement area is larger than minimum requried reinforcement area:

To check the moment capacity of this design:

After verifying the bending moment capacity, the shear capacity of the concrete should be assessed to determine if additional shear reinforcement is required.

Table B.6.: Reinforcement area check

Side	Minimum area for reinforcement	Designed area for reinforcement	Reinforcement
Excavation Side	$A_{s,min} = 903mm^2$	2094 mm^2	@20-150mm OK!
Ground Side	$A_{s,min} = 615mm^2$	$997mm^2$	@20-315mm OK!

Table B.7.: Moment Capacity for the Reinforcement Design

Side	Condition	Design Bending Moment	Bending Moment Capacity	Reinforcement
Excavation Side	ULS	−350 kNm	-422 kNm	@20-150mm OK!
Ground Side	ULS	125 kNm	232 kNm	@20-315mm OK!

As illustrated in Figure B.15, the shear resistance check, represented by the blue and red lines ($V_{Rd,c}$), is greater than the design shear force. Consequently, under these conditions, no additional shear reinforcement is required.

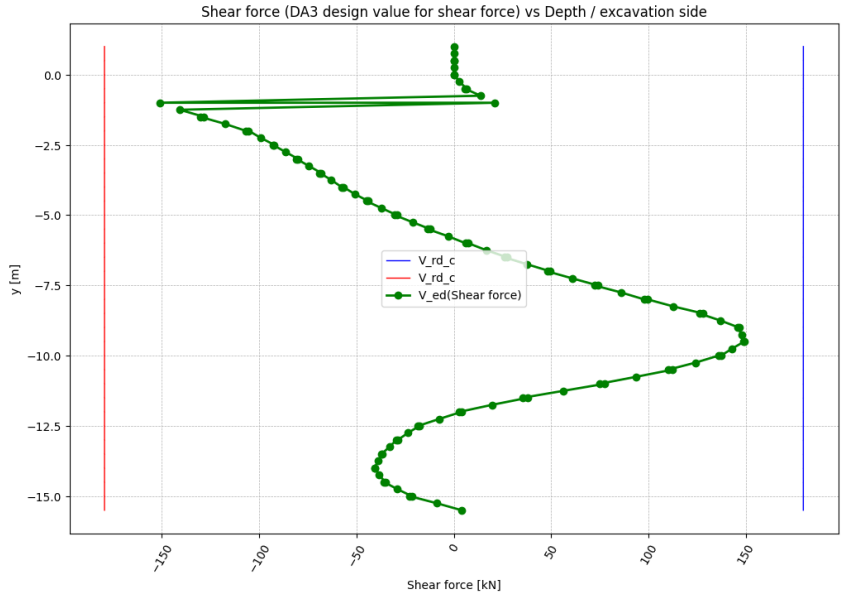

Figure B.15.: Shear force check

- Serviceability limit state check

After verifying the ULS reinforcement design, the crack width for SLS scenrio is conducted.

Table B.8.: Crack width for the Reinforcement Design

Side	Condition	SLS bending moment	Normal force	Crack width w_k
Excavation Side	SLS	−260 kNm	-193 kN	0.29mm $<$ 0.3mm OK!
Ground Side	SLS	92 kNm	-198 kN	0.29mm $<$ 0.3mm OK!

Therefore, as shown in Table B.8, the crack width meets the Serviceability Limit State (SLS) requirements. The design is OK; Table B.9 shows the final design.

Following the verification of both ULS and SLS designs, a unity check is performed to determine which design governs, SLS or ULS.

- Unity check

Table B.9.: D-wall Final Design for Case Study

D-wall Design	
Thickness	**0.5m**
Concrete type	**C35/45**
Reinforcement Design	
Minimum required coverage C_{min}	**45mm**
Applied coverage C_{nom}	**50mm**
Excavation side reinforcement	**@20(150mm)**
Ground side reinforcement	**@20(315mm)**

Table B.10.: Unity check for the Reinforcement Design

Condition	Unity check
Excavation side	
ULS	0.82
SLS	0.97 Govern!
Ground side	
ULS	0.54
SLS	0.97 Govern!

After completing the unity check, to decide the design governed by the Serviceability Limit State (SLS) is finalized for this scenario.

B.4. Six soil element behavior

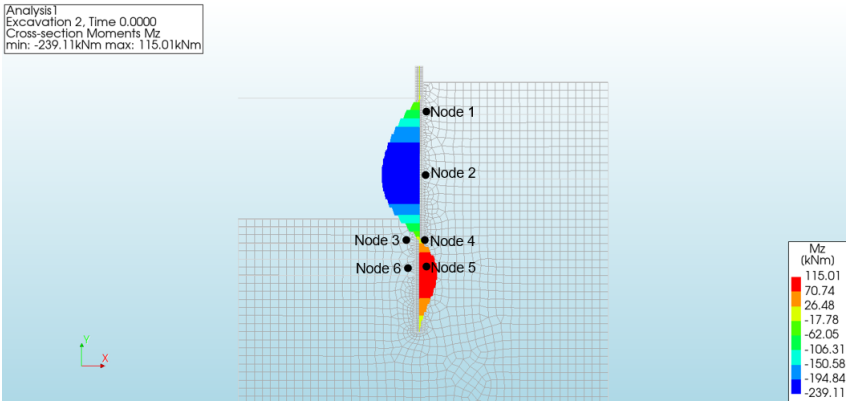

Figure B.16.: Six elements selection for the analysis soil behavior

- Node 1 location: X=11,58m Y=-0,33m

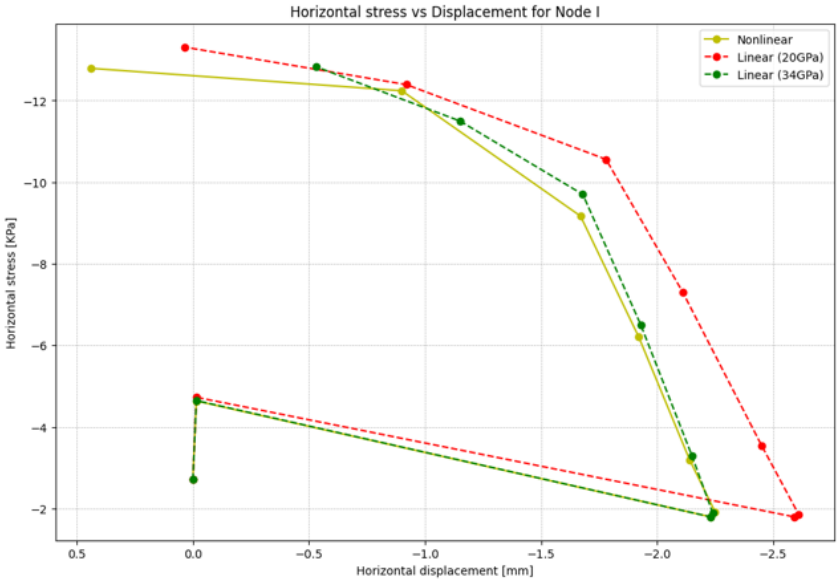

Figure B.17.: Node 1 behavior

As Figure B.17 shows that the relationship between the horizontal stress of the soil and the horizontal displacement, before the strut is installed, the soil undergoes unloading. Once the strut is applied, the soil begins to experience loading. Because the strut prevents the upper part of the D-wall from tilting to the left. There shows the almost the same trend for the three analysis, but slight difference for value result.

- Node 2 Location: X=11,6m Y=-5,43m

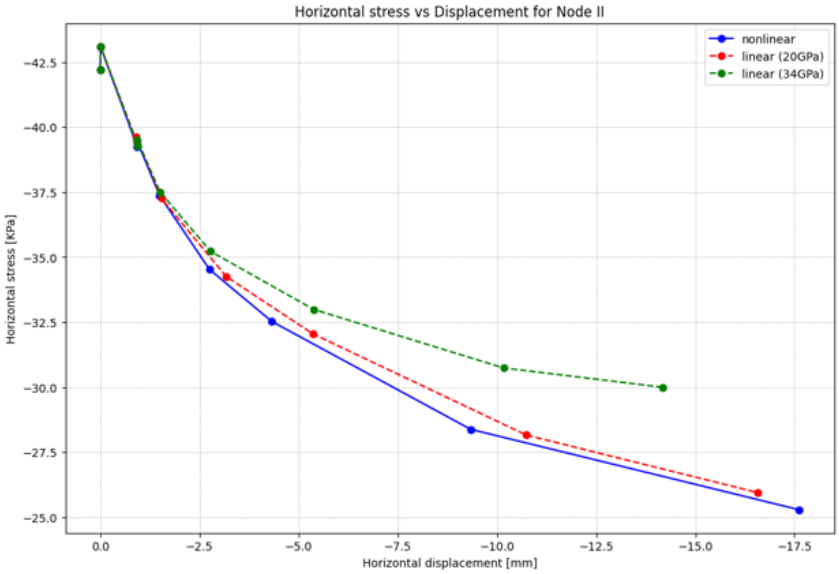

Figure B.18.: Node 2 behavior

From the Figure B.18, to know that soil element 2 is located below the strut and above the excavation. It continues to undergo unloading and, as the trend indicates, is approaching stable behavior, with the information in Figure 3.6 showing that the soil element 2 is approaching failure. Same as the Node 1, the results shows the almost the same trend for the three analysis, but slight difference for value result.

- Node 3 Location: X=10,5m Y=-10m

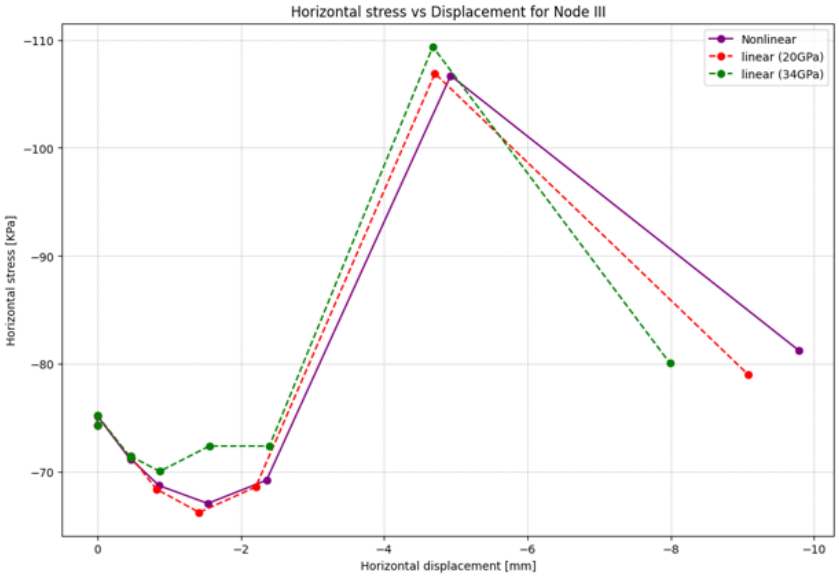

Figure B.19.: Node 3 behavior

Soil element 3 is located in the final zero bending moment zone on the excavation side. In the Figure B.19 shows the abrupt jump for the horizontal stress change indicates that the zero-bending moment point shifts throughout the construction process. Still same as the Node 1 and Node 2 result, the very small difference for value result between three analysis.

- Node 4 Location: X=10,5m Y=-10m

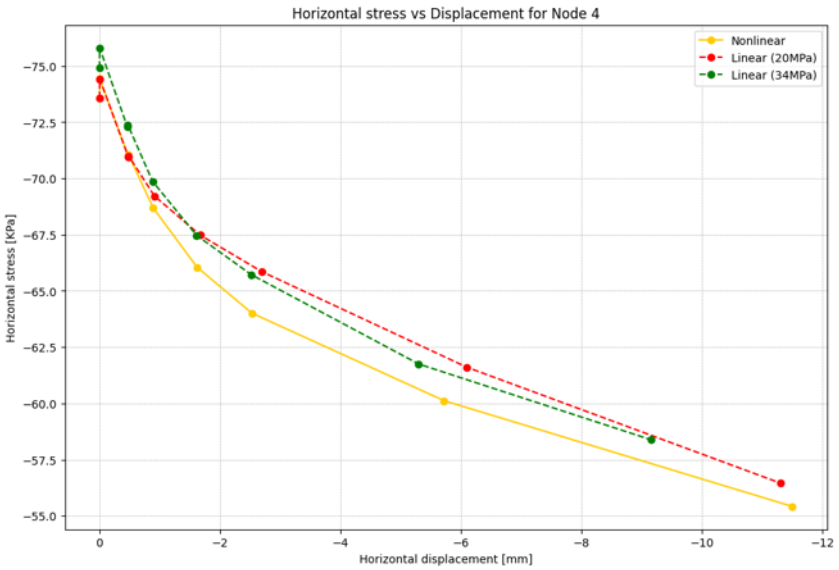

Figure B.20.: Node 4 behavior

At the same depth as Node 3 but in the different side of D-wall, Figure B.20 indicates the Node 4 continues to undergo unloading, and the displacement is almost the same as the Node 3. Consistent with the nodes before, not big difference between the three analysis, shows almost the same behavior for the soil elements.

- Node 5 Location: X=11,54m Y=-11,69m

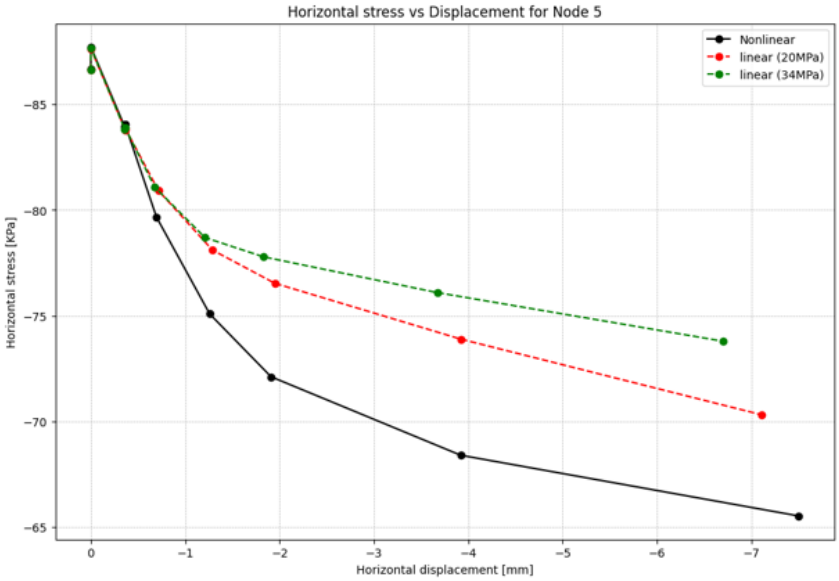

Figure B.21.: Node 5 behavior

From Figure B.21, which illustrates the soil behavior throughout the construction process for Node 5, it can be seen that Node 5 continues to experience unloading since it is located below the strut. As the D-wall continues to incline towards the excavation side, this causes ongoing unloading of the soil at Node 5. While all three analyses show the same trend in soil behavior, there are significant differences in the values, with noticeable variations between the analyses:

The green line (34GPa) linear concrete analysis, shows the least displacement and largest horizontal stress.
The red line (20GPa) linear concrete analysis, shows the moderate displacement and horizontal stress.
The black line (34GPa) nonlinear concrete analysis, shows the least displacement and least horizontal stress.

The results from the three analyses reveal consistent patterns for wall displacement and bending moment distribution. However, Node 5 more clearly highlights the differences between the analyses, likely because it accumulates the effects of the soil-structure interaction from above.

The results for Node 5 show that the nonlinear analysis produces greater soil displacement, which in turn triggers more soil-structure interaction. This increased interaction reduces soil pressure, which helps lower the bending moment, ultimately benefiting the reinforced-concrete design.

- Node 6 Location: X=10,89m Y=-11,68m

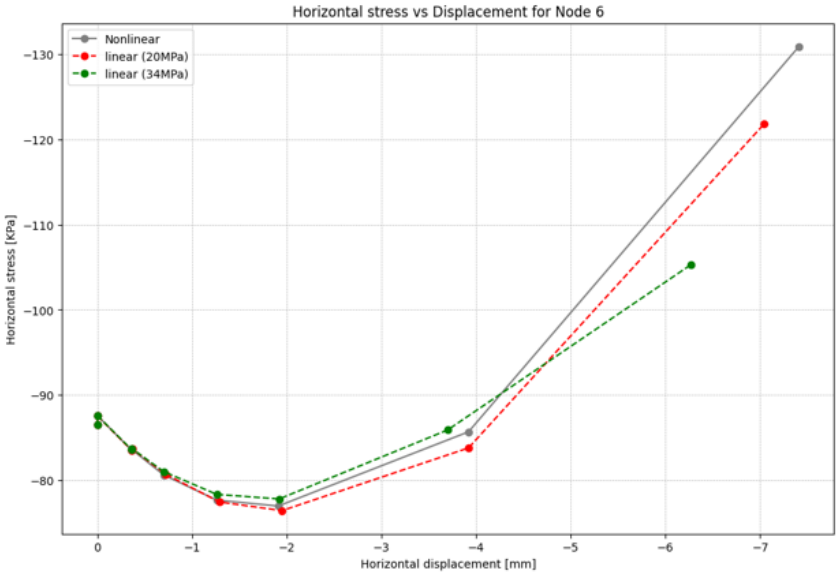

Figure B.22.: Node 6 behavior

Node 6 located at the same depth as Node 5 on the different side of the wall D (excavation side), but the differences between the three analysis are not as big as Node 5 shown in Figure B.22, the displacement of Node 5 and 6 is almost the same, because they were placed at the same depth, but the soil reflect different, as the soil is a continuum material that could be influenced by their neighbor soil, leading to the different reflection and the slight difference in the result of the value.

C. Appendix: Practical case model

As demonstrated in Chapter **??**, the methodology for linear concrete analysis employs the linear-elastic model to simulate concrete behavior. For the soil constitutive model, the Hardening-Soil model is used. Detailed indexes are provided in Chapter **??**. The aim of linear analysis first is basic verification the finite element model's correctness and stability. Once the linear concrete model is successfully convergence each construction step in Diana, then the concrete model can be converted to non-linear model. Secondly, the linear model helps to understand the basic reaction of the D-wall, providing insight for further nonlinear concrete analysis.

C.1. Boundary condition and Mesh

Based on the Chapter **??** simplified symmetrical model to build the Finite element model in Diana, shows as Figure C.1 shows the first step of construction and end of the construction and the red arrow in the FigureC.1 illustrate the support (boundary condition) in the model. And as Figure C.2 shows, the mesh generation for the modelling. And Table C.1 shows the details of the mesh size for different element use in the model.Due to the complexity of this model compared to the case study scenario, performing a mesh test for different mesh sizes is challenging. Considering the time required for model analysis, a relatively large mesh size was used for the undisturbed soil to reduce computation time. To ensure accurate loading results for the D-wall, a mesh size of 0.2m was chosen for the D-wall, while a 0.4m mesh size was applied to the removed soil, balancing accuracy and efficiency in the analysis.

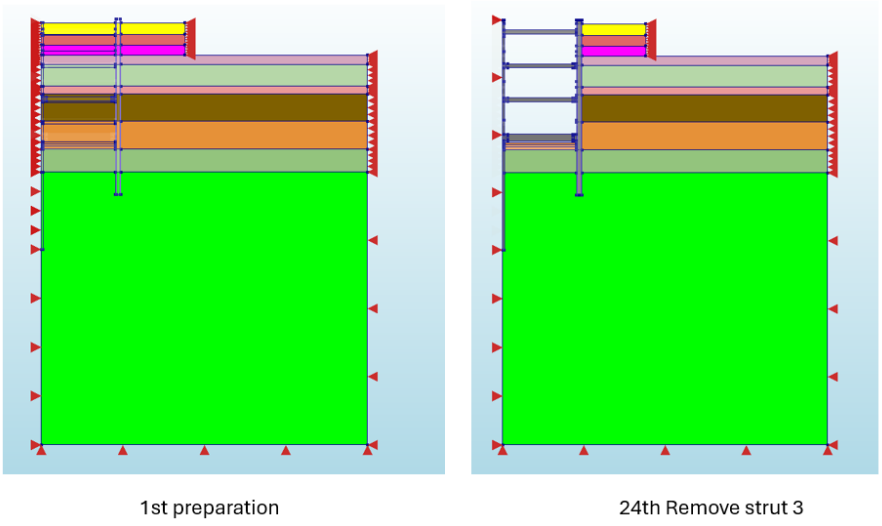

Figure C.1.: Finite element model for first and end step of construction

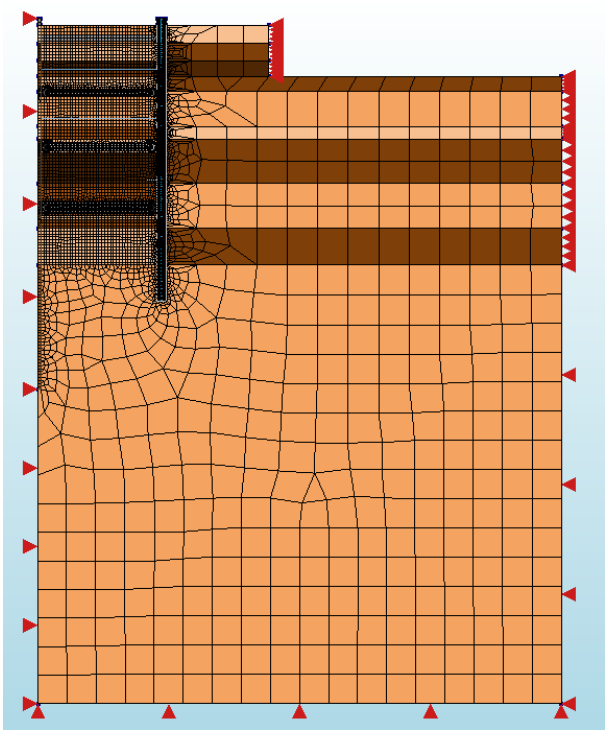

Figure C.2.: Generation the mesh for first and end step of construction phase

Table C.1.: Mesh size for different element

Element type	Mesh size
D-wall	0.2m
Excavated soil	0.4m
Not excavated soil	4m

To ensure the accuracy of the linear analysis model, the displacements at each step are thoroughly analyzed. However, for the bending moment, normal force and shear force, only the critical step is considered, the final construction step. The bending moment, normal force, and shear force diagrams from this step are used to inform the next phase of reinforcement design.

C.2. Iteration and load step

C.2.1. Iteration selection

Following the same process as outlined in Chapter 3, different iteration counts were tested. However, due to the complexity of this analysis and the associated computational costs, stability of the results is a key consideration. Therefore, the optimal number of iterations was selected to balance time efficiency and computational stability.

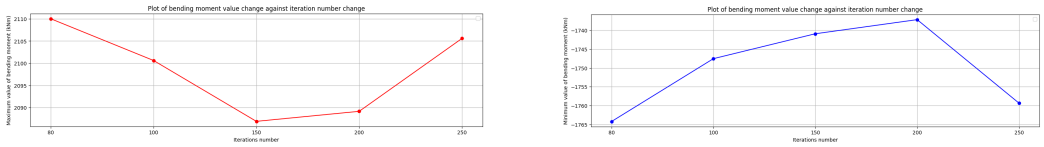

(a) Max.(bending moment result) change against iteration number change

(b) Min.(bending moment result) change against iteration number change

Figure C.3.: Bending moment result change againist iteration number change

As the Figure C.3, combine the result change with increase of iteration number, when the iteration number is 150 the maximum and minimum bending moment is stay relative stable, compared to other iteration number applied in the analysis. Therefore, to choose the 150 as the iteration number for the analysis.

C.2.2. Load step

In this scenario, the load steps for each construction stage differ from those in the case study, where the excavation was based on hypothetical conditions. The case study used varying load steps to ensure stability and accuracy in the analysis. However, in this scenario, the load steps are directly related to the construction timeline, with each step influencing the overall time cost for different stages of the project.

C.2.3. Convergence norm

The convergence norm for displacement and force balance is chosen to be 0.01. This norm can provide sufficient accuracy for finite element modeling, indicating that the results are close to the exact solution. Using a stricter convergence norm would lead to more iterations and higher computational resource consumption, which is unnecessary for the model's required precision.

C.3. Hinged connection

C.3.1. Tension cut-off interface

As discussed in Chapter **??**, there are two ways to simulate the hinged connection for floor -1, floor -2 and bottom floor. The first method is using tension cut-off interface element to model the hinged connection. The hinged connection index listed in the Chapter **??**.

Based on the behavior of the hinged connection, there is no bending moment transfer at the connection. However, the results (after the application of the bottom floor phase) shows at each connection point there will be a noticeable increase in bending moments, potentially resulting in a peak, which indicates that the tension cut-off interface element does not prevent bending moment transfer between the floor and the diaphragm wall (D-wall). When the floor is relaxed, the tension cut-off interface behaves like a hinged connection. However, once the horizontal load increases, the tension cut-off interface can no longer rotate freely, resulting in bending moment transfer from the floor to the D-wall.

Figure C.4.: After bottom floor applied bending moment for tension cutoff interface model the hinged connection

C.3.2. Geometry method

Therefore, the interface element method is replaced with the geometry method to achieve the hinged connection behavior. The modified geometry method used to simulate the hinged connection is shown in Figure C.5. The right section of the floor is unified with the D-wall, while the left section is separate from the right section. An interface exists between the left and right sections of the floor, the index shows in Chapter **??**.

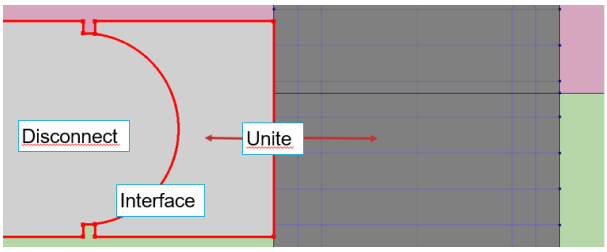

Figure C.5.: Geometry way of hinged connection

After applied the geometry method to simulate the hinged connection, the bending moment of the composed line result shows in Figure C.6. After modifying the hinged connection using the geometry method, there is a reduction in bending moments at each floor and D-wall connection. This indicates that the bending moment transfer has decreased, proving the modification to be highly effective compared to the tension cut-off method. The geometry method simulation of hinged connection is determined to simulate the hinged connection.

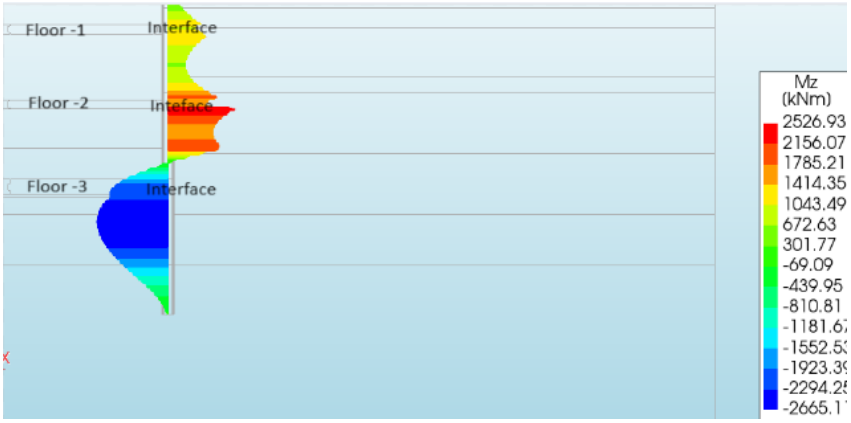

Figure C.6.: After the bottom floor applied using geometry way to simulate hinged connection

C.4. Phased displacement result analysis

To verify the accuracy of the model and correctness of element properties, phased displacement results are crucial. Therefore, for the first step analysis, phased displacement result prioritized for analysis. The following construction step are important within the overall construction process, including stages with significant displacement and the addition of new element.

C.4.1. Stage 1: Preparation displacement result

Based on the construction stages, a phased analysis should be conducted. For the whole system, both horizontal and vertical displacements should be analyzed. Several stages need to be emphasized, including the first and last stages, the drainage stage, and the stages related to floor application (induce big displacement stage), which require additional attention and check. Because the first stage as Figure C.7 shows which is before the application of D-wall, so it is reasonable to be static and no change for the first construction step.

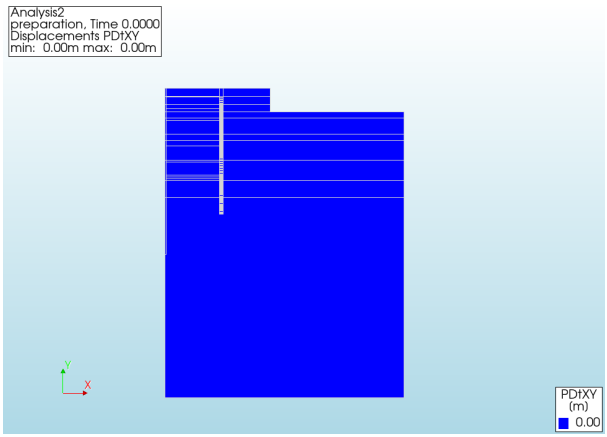

Figure C.7.: First step displacement (before applied the D-wall)

C.4.2. Stage 2: Pre-consolidation displacement result

After pre-consolidation of sand,the soil most downwards -160.41mm, and for the X-direction there is no big displacement.

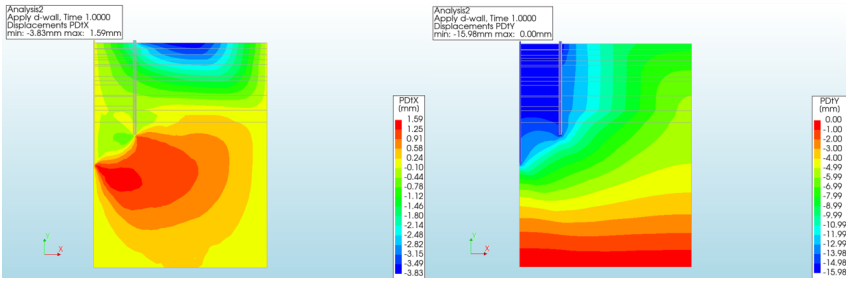

Figure C.8.: Apply the D-wall displacement result

C.4.3. Stage 3: Apply D-wall

After pre-consolidation, the soil becomes more compact, resulting in increased stiffness. Consequently, when the D-wall is installed, the soil displaces upward by 47.78 mm as Figure C.9 in the Y-direction, while the horizontal displacement remains minimal.

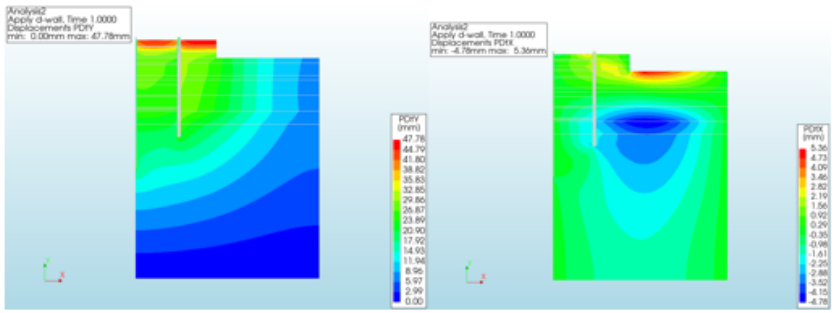

Figure C.9.: Step 3: Apply D-wall displacement result

C.4.4. Stage 4: Excavation to -2.8m + drainage

For the next step is a bit special because it's combine the first drainage and excavation step together. Therefore, it should be pay more attention to the displacement result.

As shown in Figure C.10, the horizontal displacement is quite small. For the vertical displacement, it is reasonable for the soil and wall to experience upward displacement due to the excavation of sand, with the value of 35.69mm upwards. Thus, the phase displacement for this stage is quite reasonable.

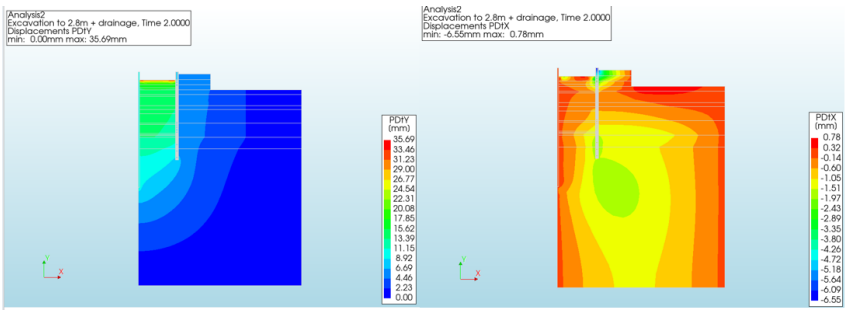

Figure C.10.: Step 4: Excavation to -2.8m + drainage

C.4.5. Stage 5: Grout soil

The next construction step involves grouting the bottom sand layer. As shown in Figure C.11, this grouting process causes the soil above to settle, with a downward displacement of -68.16 mm. In the X-direction, the soil beneath the grouted layer experiences a leftward movement with the value of -15.43 due to the soil improvement, thus the upper part is experienced right side movement with the value of 6.18mm.

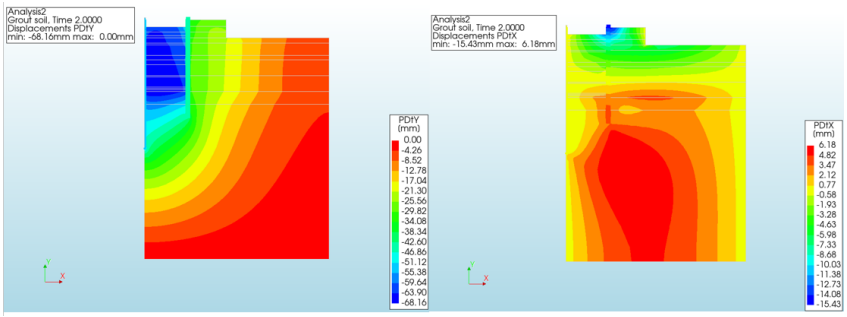

Figure C.11.: Step 5: Grout soil stage displacement result

C.4.6. Stage 6: Install strut 1

To verify the accuracy of the strut properties, the phase displacement during the installation of the strut is analyzed. Figure C.12 illustrates the phase displacement after the first strut is installed. In both the X and Y directions, the displacements are minimal due to the relatively low mass of the strut.

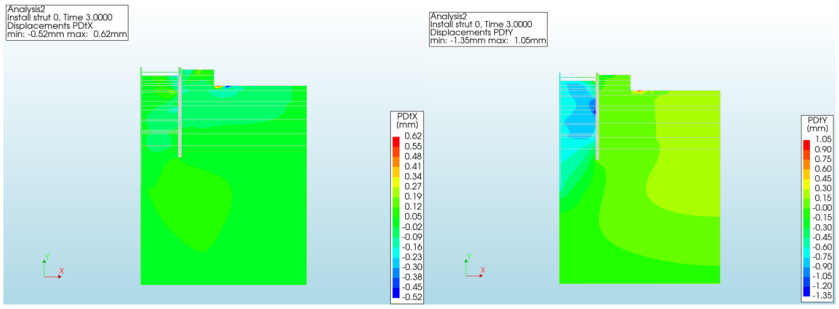

Figure C.12.: Step 6: Install strut 1 displacement result

C.4.7. Stage 11: Apply floor -1 displacement result

Besides the strut element, there is another new element requires attention is floor. Therefore, the initial step of adding the floor is crucial to verify its properties. The property of the floor is same as the linear D-wall analysis property, which is liner concrete property. Upon application of the floor, the middle of floor experience downwards movement due to the gravity of the floor, and the X direction displacement is small within the 2mm movement. Figure C.13 demonstrates that the overall system displacement aligns with expectations.

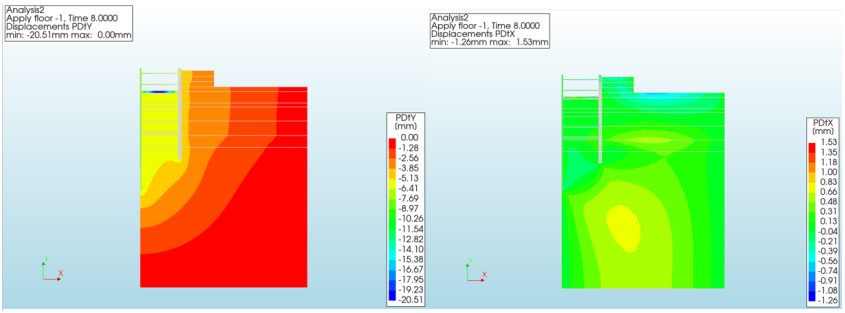

Figure C.13.: Step 11: Apply floor -1 displacement result

C.4.8. Stage 24: Remove strut -3 displacement result

After checking the critical step for the construction process, the phased displacement result for end construction stage is shown in Figure C.14.

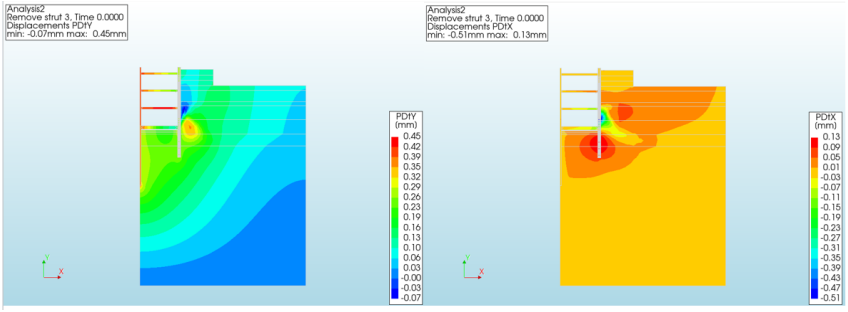

Figure C.14.: Step 24 (end phase): Remove strut 3 phased displacement result

At this stage, the strut is removed, resulting in the loss of normal force that supports the D-wall. However, the influence of the sturt is relatively small, lead to very small displacement result in both X and Y direction.

C.5. Final result analysis

Once the method to simulate the hinged connection was determined, verification of the phased displacement results followed. Each construction and load step, except for the initial preparation in step 1, converged successfully. This validates the accuracy of the simulation and confirms the model's successful running. Detailed discussion of the simulation results for the first step will be provided in the later section.

C.5.1. Bending moment result of D-wall

As Figure C.15, at the last construction step, the bending moment diagram of composed line.

- Bending moment result analysis:

Based on the bending moment diagram result, there have 2 peaks in this diagram, first peak is between the floor -2 and -3 with the value of -1737.6kNm, and the second peak is under the excavation surface with the value of 2089.15kNm. At the base, the bending moment is very small which shows the stable of D-wall.

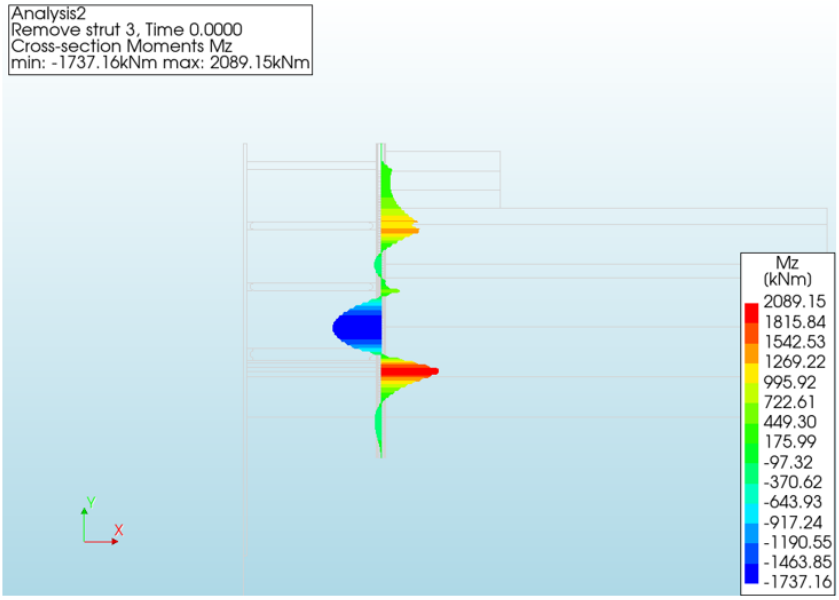

Figure C.15.: Bending moment diagram for D-wall

C.5.2. Normal force result of D-wall

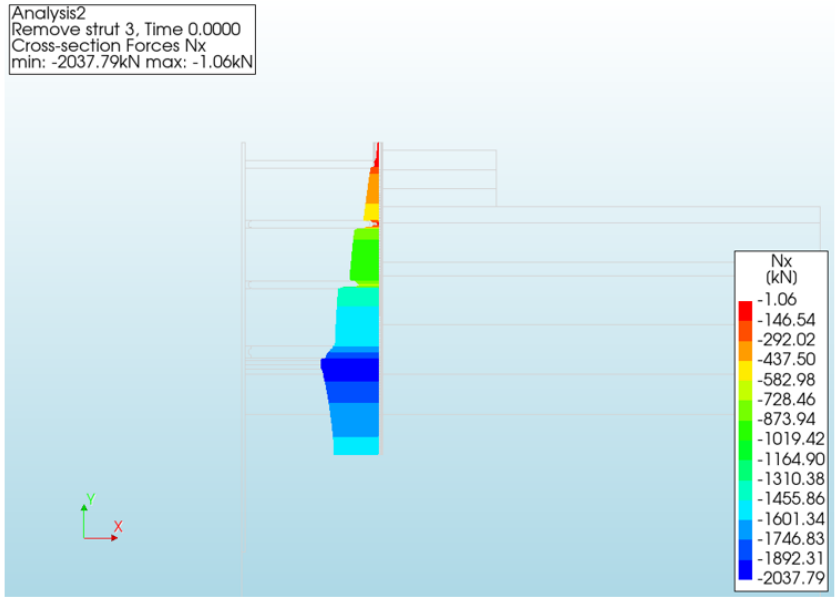

Figure C.16.: Normal force diagram for D-wall

Figure C.16 illustrates the variation of normal force along the D-wall, showing an increase from the top of the wall down to a depth of -20.43m, which corresponds to the depth of the deep excavation. The maximum normal force reaches -2037.07 kN. The intervals in the normal force line at each floor's D-wall connection are due to errors caused by the composed line. The section C.6 will be detailed discuss of composed line error.

C.5.3. Shear force result of D-wall

Figure C.17 shows the shear force diagram along the D wall, which shows the minimal value of -1045.13kN at depth around -11.4m, which corresponds to the bottom of floor -2. And the maximum value of shear force occurs at the depth around -21m which corresponds to the bottom floor.

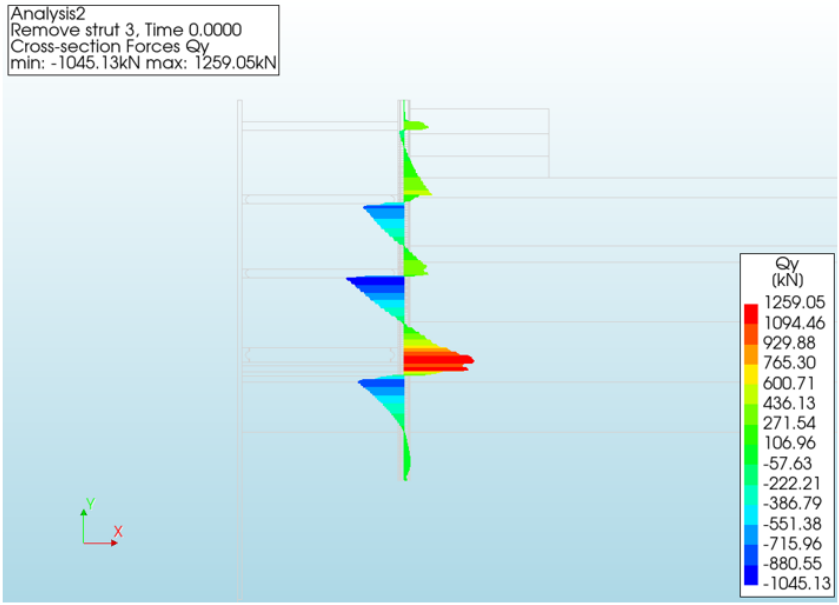

Figure C.17.: Shear force diagram for D-wall

C.6. Discussion

C.6.1. First construction step divergence

As mentioned above, all the construction steps except the first step have converged. The divergence in the first step is due to displacement variation, while force balance has already achieved convergence in the first step.

The reason for the divergence in the preparation phase is primarily because the geometry of the model is not symmetrical as Figure C.17 shows it apparently not symmetrical which is the phase after apply of D-wall, making it difficult to achieve convergence without any applied forces. Therefore, the convergence of force balance is crucial for the first step. Once force balance is achieved, the first step can be considered converged.

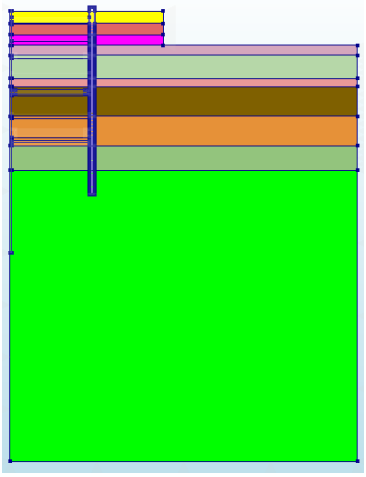

Figure C.18.: Asymmetrical of model

C.6.2. Composed line impact

As the chapter **??** introduces the composed line element, the composed line element function demonstrates how a cross-section of the model can be computed using a line defined with composed line elements. These elements can generate local internal forces and bending moments relative to the reference line.

However, in this modeling approach, the composed line elements are generated only with a defined thickness equal to the D-wall thickness as Figure shows C.19 the thickness is 1.2m. As a result, other parts that are unified with the wall are ignored, leading to errors in the diagrams, such as the normal force diagram. This occurs because the composed line elements do not account for the thickness of the floor console. Like in Figure C.19, the edge of the console and D-wall thickness should be 1.95m instead of 1.2m. To correct the normal force diagram, the normal force line should be a continuous straight line without intervals or breaks in between.

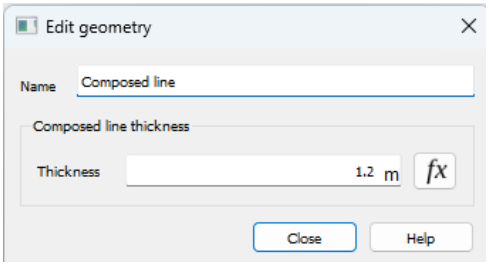

(a) The composed line geometry information

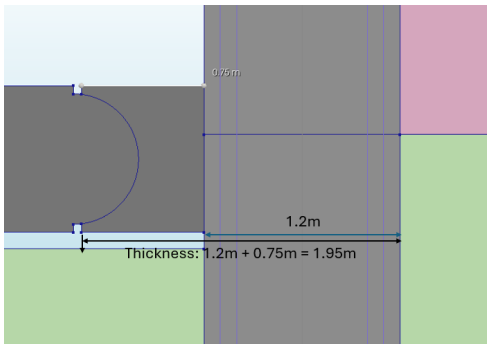

(b) The console thickness ans D-wall thickness

Figure C.19.: The composed line and console information

C.7. Conclusion

The linear analysis uses reduced concrete stiffness, typically 60 percent of the original, to simulate concrete cracking. In DIANA, the total displacement result is not continuous, so phased displacement results are used for the analysis. The shear force, normal force, and bending moment distributions from the final phase are chosen as representative loading conditions. Based on the results from this reduced-stiffness linear analysis, the reinforcement design is then conducted.

As shown in the linear analysis bending moment results, the peak value occurs on the ground side of the D-wall. As discussed in Chapter 3, cracks should be avoided on the ground side, as water in the soil can cause reinforcement erosion. Therefore, conducting a nonlinear analysis to assess potential cracking in the D-wall is crucial.

And for the hinged connection, it is clearly that the geometry way provide more reality model compared to the tension cut-off surface, therefore, the latter simulations continues using the geometry way to model hinged connection.

C.8. Reinforcement design

After running the linear analysis, the bending moment, normal force, and shear force results were obtained from Diana. As discussed in Chapter 2, both the Ultimate Limit State (ULS) and Service Limit State (SLS) should be checked following the same process as in Chapter 3. Table C.2 presents the reinforcement design used for this D-wall, which would used for conducting the ULS and SLS checks.

Table C.2.: D-wall design

D-wall Design	
Thickness	**1.2m**
Concrete type	**C35/45**
Reinforcement design	
Tunnel side	**283mm@50+283mm@40**
Ground side	**283mm@40+283mm@50**
Shear reinforcement	**150mm@12**

C.9. Ultimate limit state check

First, to decide the ultimate limit state design load in this scenario, for the favourable loading, the safety factor is 1, and for the unfavourable loading, the safety factor is 1.35. The process is same as the Chapter 3 to calculate the design load, and check the moment capacity for the D-wall design.

C.9.1. Ultimate limit state design load

- Design bending moment

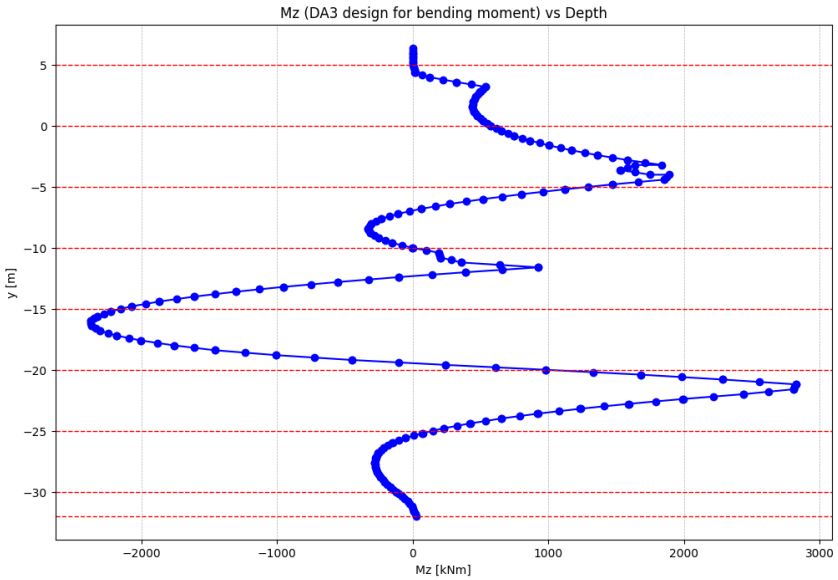

Figure C.20.: Design bending moment

As Figure C.20 shows, after applied partial factor to the bending momet, the maximum value of design bending moment is 2828 KNm, and the minimum value of design bending moment is -2324 KNm.

- Design shear force

Figure C.21 illustrates the design shear force for ULS, and the maximum shear force is 1711 KN, and the minimum shear force is -1413 KN.

- Design normal force

Because the normal is favorable for the design, the partial factor for the favourable part is 1. Thus, the normal force stay same as the analysis result. As Figrre C.22 shows the ULS design normal force.

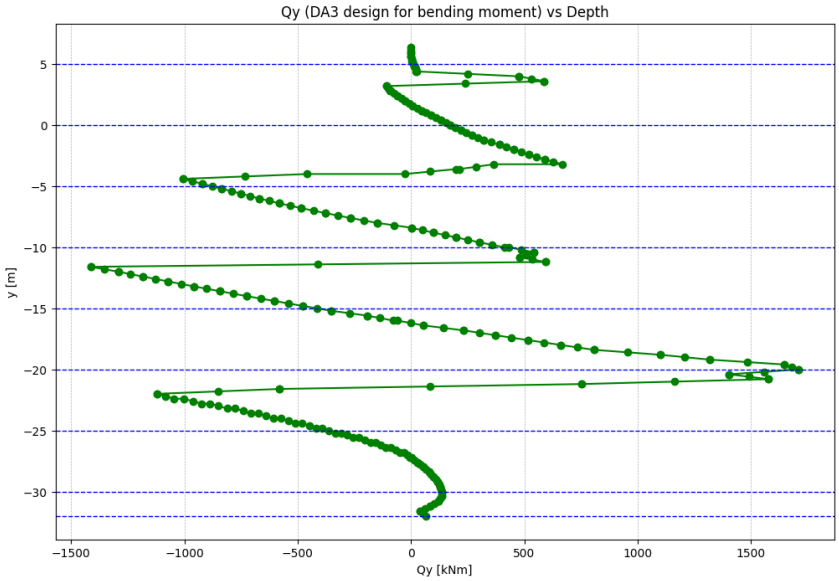

Figure C.21.: Design shear force

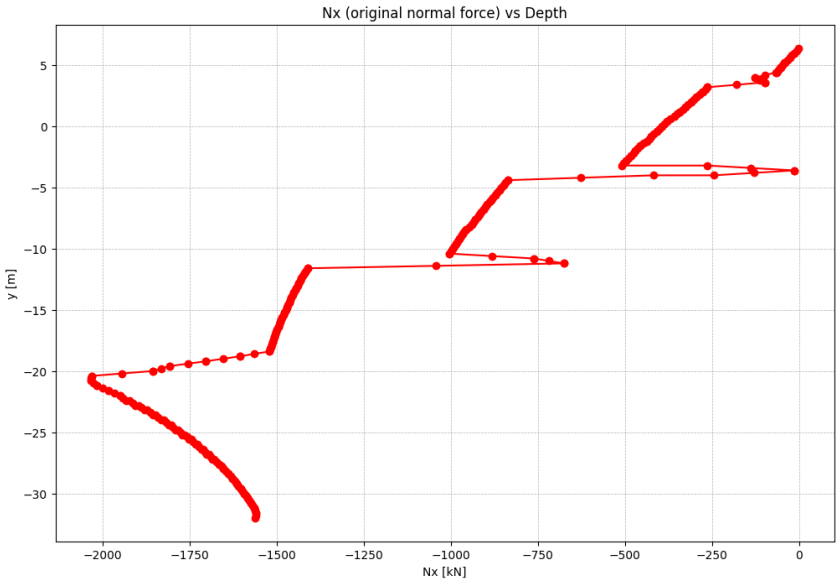

Figure C.22.: Design Normal force

C.9.2. Ultimate limit state check

- Minimum area check

Table C.3.: Reinforcement Area Check

Side	Min. Area (mm^2)	Designed Area (mm^2)	Reinforcement
Tunnel	2865	10025	283@50+283@40OK!
Ground	3004	10050	283@40+283@50OK!

- Moment capacity check

- Shear force check

Table C.4.: Moment Capacity Check

Side	Cond.	Design Moment (kNm)	Capacity (kNm)	Reinf.
Tunnel	ULS	-2324	-4570	283@50+283@40OK!
Ground	ULS	2827	4738	283@40+283@50OK!

To plot the $V_{rd,c}$ in the Figure C.23 , to show the $V_{rd,c}$ from 3m to -25m is smaller than the designed shear force for the D-wall for both sides (the longitudinal reinforcement areas in very close), therefore, the shear reinforcement is required for this section.

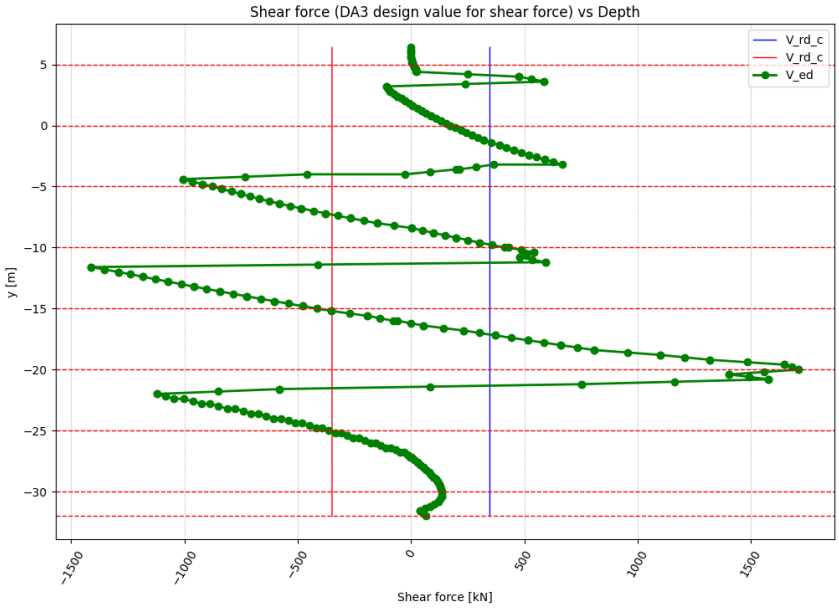

Figure C.23.: Resistance shear $V_{rd,c}$ vs Design shear force V_{ed}

And to calculate the reinforcement area required for the shear resistance, the final shear reinforcement design:

Table C.5.: Shear reinforcement design

D-wall depth (m)	Shear reinforcement
3-0	275mm-@20
0- (-10)	150mm-@20
-10 - (-15)	100mm-@20
-15 - (-20)	250mm-@20
-20 - (-25)	150mm-@20

C.9.3. Serviceability limit state check

As shown in Table C.6, the crack width check for this scenario corresponds to an environmental condition of XC2, where the maximum allowable crack width is 0.3 mm.

Table C.6.: Crack width for the Reinforcement Design

Side	Condition	SLS bending moment	Normal force	Crack width w_k
Tunnel Side	SLS	-1738 kNm	-1600 kN	0.21mm $<$ 0.3mm OK!
Ground Side	SLS	2089 kNm	-2037 kN	0.27mm $<$ 0.3mm OK!

Then to decide the final design of reinforcement for D-wall:

Table C.7.: D-wall final reinforcement design

D-wall Design	
Thickness	**1.2m**
Concrete type	**C35/45**
C_{app}	**100mm**
Longitudinal reinforcement	
Tunnel side	**283mm@50+283mm@40**
Ground side	**283mm@40+283mm@50**
Shear reinforcement	
Depth(m)	Reinforcement
3-0	275mm-@20
0- (-10)	150mm-@20
-10 - (-15)	100mm-@20
-15 - (-20)	250mm-@20
-20 - (-25)	150mm-@20

C.9.4. Unity check

Table C.8.: Unity check for the Reinforcement Design

Condition	Unity check
Tunnel side	
ULS	0.51
SLS	0.7
Ground side	
ULS	0.60
SLS	0.9 Govern!

After reviewing the D-wall design, the Serviceability Limit State (SLS) is determined to be the governing design criterion in this scenario.

C.9.5. Crack width result

In the nonlinear analysis, an additional result related to cracking is presented, showing the concrete cracks in both the X and Y directions, as illustrated in Figure C.24 and C.25. However, this crack-width result does not account for slip cracks, which would require post-analysis. In this plot, cracks appear on both sides of the wall, occurring at the locations where the bending moment peak values are observed.

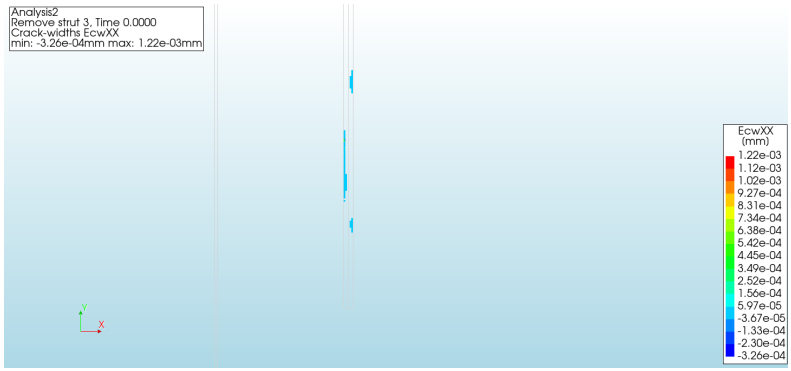

Figure C.24.: Crack width X-direction

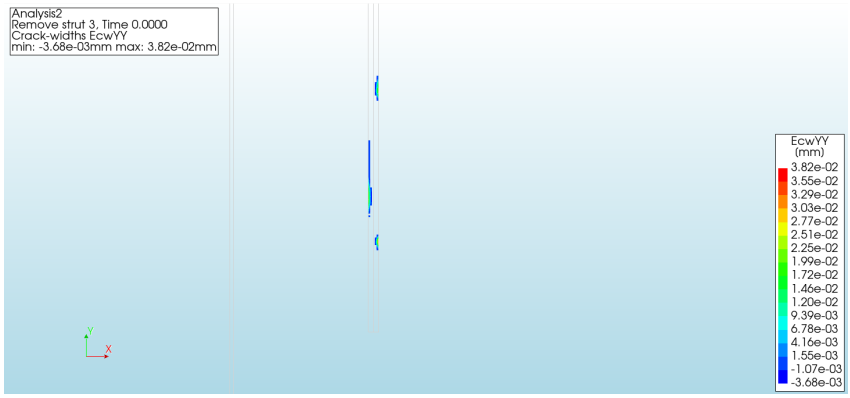

Figure C.25.: Crack width Y-direction

However, it should be noted that cracks occur on the ground side of the D-wall. As discussed earlier, cracks on the ground side should be avoided to protect the reinforced concrete from potential erosion, particularly from water infiltration. Therefore, this aspect of protection for the reinforced concrete will be addressed in further detail later.

C.9.6. Reinforcement stresses and strain result

Figure C.27 illustrates the total reinforcement stress in the Y direction. The areas of higher stress correspond to the locations of peak bending moments, with stress values reaching -43.23 MPa and 40.80 MPa. Given that the concrete's compressive strength is 23.3 MPa, these stress levels exceed the concrete's capacity, resulting in cracking. The peak reinforcement strain values are -2.19e-04 and 2.04e-04, occurring at the same locations as the peak stress as Figure C.27 shows.

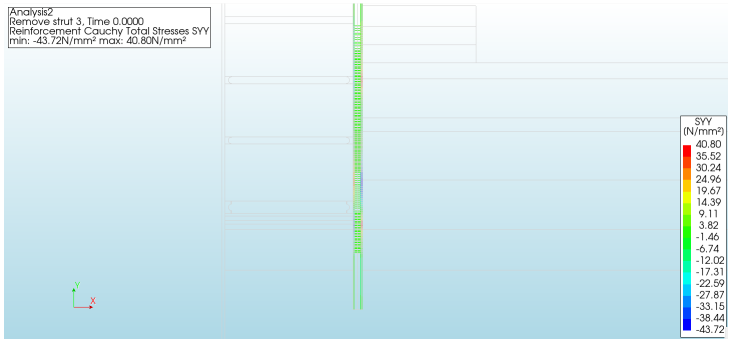

Figure C.26.: Total stress for reinforcement result

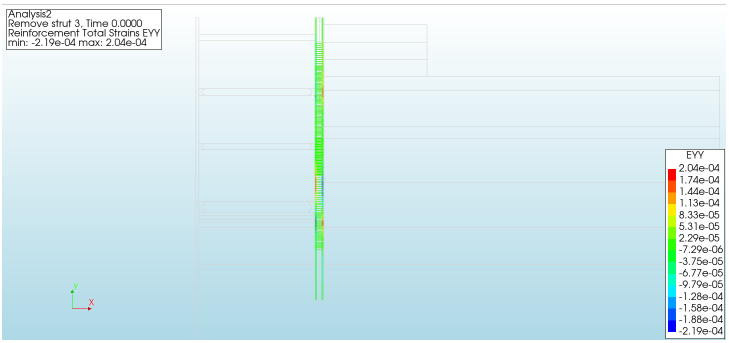

Figure C.27.: Strain for reinforcement result

C.10. Conclusion

In the complex scenario, which is significantly more intricate than the case study, several key differences are observed. This scenario includes 13 distinct soil layers, the presence of groundwater, 3 struts, and 4 floors. Each floor interacts differently with the D-wall: the first floor has a fixed connection, while the other floors are hinged. Additionally, the construction process involves 23 steps, making the analysis much more challenging than in the simpler case study. Despite this complexity, the bending moment distribution results from the three analyses remain consistent with the case study, demonstrating that the theory derived from the case study can be applied to this more complex scenario.

From the results of the three analyses, it is clear that the D-wall experiences high pressure in this scenario, making cracks inevitable, even with the use of large reinforcement. Cracks are observed on both sides of the wall in the nonlinear analysis results. Comparing the three analyses reveals that the nonlinear analysis results closely align with the bending moment results of the reduced-stiffness linear concrete analysis. This suggests that the nonlinear analysis has limitations in refining the reinforced concrete design if considered solely based on bending moment distribution.

However, from the soil pressure results, there is still potential to trigger more soil-structure interaction, which could help reduce soil pressure and ultimately benefit the reinforced concrete design. This indicates that further refinement could be achieved by focusing on the soil-structure interaction in addition to the bending moment distribution.